BIOELECTROCHEMICAL REMEDIATION OF NITRATE CONTAMINATED GROUNDWATER IN MICROBIAL FUEL CELL

By

Hanyu Tang

A thesis submitted in partial fulfillment of

the requirements of the degree of

Master of Science

(Civil and Environmental Engineering)

at the

UNIVERSITY OF WISCONSIN-MADISON

2022

Abstract

Nitrate contamination in groundwater is a growing concern in Wisconsin, due to the increasing concentration in groundwater sources and its intensive application as a fertilizer for agricultural activities. In addition, most people in rural regions rely on groundwater as their primary supply of drinking water. There is increasing interest in groundwater nitrate removal. Traditional in-situ nitrate removal methods include reverse osmosis (RO) and ion exchange resin both of which have a high removal efficiency but are costly for decentralized in-situ treatment. Microbial fuel cell (MFC) is considered as a sustainable and efficient technology for nitrate removal from groundwater. However, in previous studies, groundwater is usually used as the anolyte, which potentially introduces bacteria and other ions into the treated groundwater that requires post-treatment. In this study, we designed a dual-chamber MFC system to remove nitrate ions from groundwater. Groundwater served as the catholyte, and the nitrate ions transported across the anion exchange membrane before being reduced by microorganisms. The system performance was evaluated under different conditions including varying influent nitrate concentrations, chloride concentrations, and external resistance. The kinetics of denitrification in the whole system under different operation condition was computed and the fundamental theory of the system was discussed. Most experiments achieved a high nitrate removal efficiency of greater than 95% when the nitrate concentration ranged from 14 mg L^{-1} to 56 mg L^{-1} under various operation conditions. The highest nitrate removal rate showed up when the catholyte influent nitrate concentration was 56 mg L^{-1}. The removal rate of nitrate decreased from 4.77 ± 0.14 mg L^{-1} hr^{-1} to 2.41 ± 0.45 mg L^{-1} hr^{-1} as the chloride concentration increased from 142 mg L^{-1} to 710 mg L^{-1}. The nitrate removal rate remained stable though the external resistance varied. When we fed real groundwater into catholyte influent, 90.6 ± 12.1 % of nitrate was removed and the removal rate reached 5.4 ± 0.7 mg L^{-1} hr^{-1}.

List of Figures

List of Tables

Chapter 1: Introduction

Groundwater provides drinking water to approximately two thirds of people living in Wisconsin, making the state the most reliant on groundwater as a drinking water supply among US states (Mathewson et al. 2020). Nitrate (NO_3^-) contamination is a growing concern for groundwater in Wisconsin, due to the increasing concentration in groundwater source and its intensive application as a fertilizer for agricultural activities (Nitka et al. 2019). When nitrate ions reach the aqueous zone, they are unable to bind to other cations and precipitate, allowing them to exit the aqueous phase (Bijay-Singh & Craswell, 2021). Nitrate indirectly produces health hazards by reduction to toxic nitrite in the human digestive system. Moreover, when exposed to high levels of nitrate, infants are susceptible to developing methemoglobinemia, a dangerous condition that excess nitrate interferes with the blood's ability to carry oxygen (Fewtrell 2004, Kapoor and Viraraghavan 1997). To minimize the adverse health impacts of nitrate, USEPA set the maximum contamination level (MCL) for NO_3^--N at 10 mg L^{-1} in drinking water. High nitrate concentration also is linked to colorectal cancer, thyroid disease, and central nervous system birth defects (Ward et al., 2018). Unfortunately, according to the 2020 Wisconsin Groundwater Coordinating Council Report to the Legislature, over 42,000 private wells in the state exceed the MCL of nitrate, necessitating treatment to satisfy basic health requirements.

The main methods to remove nitrate including reverse osmosis (RO), ion exchange resin, chemical denitrification, electrocatalysis, and biological denitrification. Reverse osmosis, which has been widely used for nitrate removal for drinking water, can reject dissolved constituents and only allow water molecules to transport across the membrane (Kang & Cao, 2012; Malaeb & Ayoub, 2011). Ion exchange process uses strongly basic anion exchange (SBAR) resin to remove nitrate ions (H. He et al., 2020). Electrodialysis, which is enabled by ion exchange membranes, needs a low chemical

demand and can achieve a higher water recovery than RO (Kikhavani et al., 2014). Electrochemical nitrate reduction, which converts nitrate ions into harmless nitrogen gas or ammonium ions by using appropriate catalysts, draws a lot of attention in the past decades (Genders et al., 1996). However, these technologies have some drawbacks. Ion exchange method including ion exchange resin, requires posttreatment for nitrate-rich brine, which cannot completely solve the problem. Chemical denitrification, mostly electrochemical denitrification, can hardly be commercialized because it is hard to control the formation of nitrite and ammonia or needs high pressure operation conditions (Rezvani et al., 2019). Biological denitrification is the most economical way to address nitrate containment for wastewater treatment instead of drinking water because posttreatment is required to prevent the microorganisms into the drinking water.

Bioelectrochemical system (BES), studied for years due to its high efficiency and sustainability, can avoid this problem efficiently using appropriate system setup (Logan & Rabaey, 2012). BES is a device that contains microorganisms that donate or accept electrons from an electrode. There are various types of BES including microbial fuel cells (MFCs) and microbial electrolysis cells (MECs) (Logan et al., 2019). Compared with MECs, MFCs do not need energy input, allowing them to reduce capital costs. The mechanism of nitrate removal in MFC systems is heterotrophic denitrification process which uses microbes to convert nitrate into nitrogen gas. Researchers have studied the use of MFC to remove nitrate for years. Tong & He used MFC with anion exchange membrane as a separator to treat groundwater as catholyte influent and the highest nitrate removal rate was 208.2 ± 13.3 g NO_3^--N m^{-3} day^{-1}. In this study, groundwater did not directly adhere to microorganisms, hence no posttreatment was required to eliminate germs as drinking water resources. Though this system configuration solves the treatment problem, other concerns remain unanswered, including as how nitrate concentration, competing ions and current generation impact system performance.

In this study, we designed a dual-chamber MFC using anion exchange membrane (AEM) as a separator and synthetic groundwater as catholyte influent. Nitrate in the influent moved to anolyte chamber and removed by heterotrophic denitrification. We investigated the nitrate removal rate under different operating conditions including varying nitrate concentrations, varying chloride concentrations and varying external resistance loadings. We also studied nitrate removal in actual groundwater. Through the study, we revealed the nitrate removal mechanism in this MFC system and how these factors affect the nitrate removal efficiency. The results are expected to provide practical insights in the development of MFC for in-situ nitrate removal from groundwater.

Chapter 2: Literature review

Nitrate in Groundwater

Groundwater is an important freshwater resource which accounts for more than 98% of the self-supplied domestic withdrawals in US, whereas 13 % of the total population needs self-supplied potable water (Dieter et al., 2017). Unfortunately, groundwater is easily polluted due to overexploitation and without recharging (Konikow, 2011). Nitrate is the most widespread containment in groundwater which contributed by nitrogenous fertilizers, organic manures, human and animal wastes and industrial effluents through the biochemical activities of microorganisms (Majumdar & Gupta, 2000). Nitrate pollution is much more serious in agriculture area than others due to the abuse of fertilizer and the emission of the manure (Hansen et al., 2017; Sahoo et al., 2016). Besides, nitrate can be generated from the ammonium and amide forms through mineralization. Due to its high solubility in water and low retention in soil, nitrate is prone to leaching to the subsoil layers and ultimately to the groundwater. The high nitrate concentration in drinking water affects human health, including blue baby syndromes and stomach cancer in adults (Almasri, 2007). The US Environmental Protection Agency (US EPA) has established a maximum contaminant level (MCL) of 10 mg L^{-1} NO_3^--N based on the concern for including methemoglobinemia in infants.

Consider Wisconsin, one of America's typical agricultural states, in south-central Wisconsin, a highly cultivated region, around 20% - 30% of private well samples exceed the MCL (Mechenich, 2015). What makes the problem worse is that the nitrate contaminant spreads through groundwater from agricultural areas affects most of the residents. Nitrate contamination is getting worse in 165 of the community water systems serving approximately 425,000 people in Wisconsin. In 2021 for the new well and pump work 9.1% of the samples were greater than 10 mg L^{-1} which exceeded the MCL set by USEPA (Wisconsin Groundwater Coordinating Council (GCC), 2022).

To protect residents from the adverse effects caused by high nitrate concentration, it is necessary to control its concentration in drinking water. Traditional chemical methods like precipitation and coagulation can hardly be used in nitrogen pollution. As a result, nitrogen removal from groundwater often involves the use of concentrate, chemical denitrification, and biological denitrification.

Nitrate removal process

The techniques for nitrate elimination are various, including reverse osmosis (RO), ion exchange, electrodialysis, electrocatalysis, and biological denitrification. Reverse osmosis (Figure 1C), ion exchange, and electrodialysis are the main methods to separate nitrate from water. Reverse osmosis (RO) rejects all kinds of ions in the water. The water goes through a semi-permeable membrane which a diameter ranging from 0.2 nm to 1 nm (Qasim et al., 2019). Nitrate can be removed under 300 to 1500 psi to reverse the normal osmotic flow of water by RO (Archna et al., 2011). Reverse osmosis has been used for nitrate treatment for over 20 years and is a common at-home drinking water treatment method. Schoeman & Steyn used RO to remove nitrate in south Africa rural areas. They achieved a high nitrate removal rate which was over 95% and relatively low water recovery. Even though RO has a high contaminant removal efficiency, several issues arise after the treatment. Three major downsides of RO include brine disposal, high operating costs, and membrane fouling. Brine produce is inevitable because RO only removes the contaminants instead of consuming them. Improper brine disposal may cause potential environmental damage such as

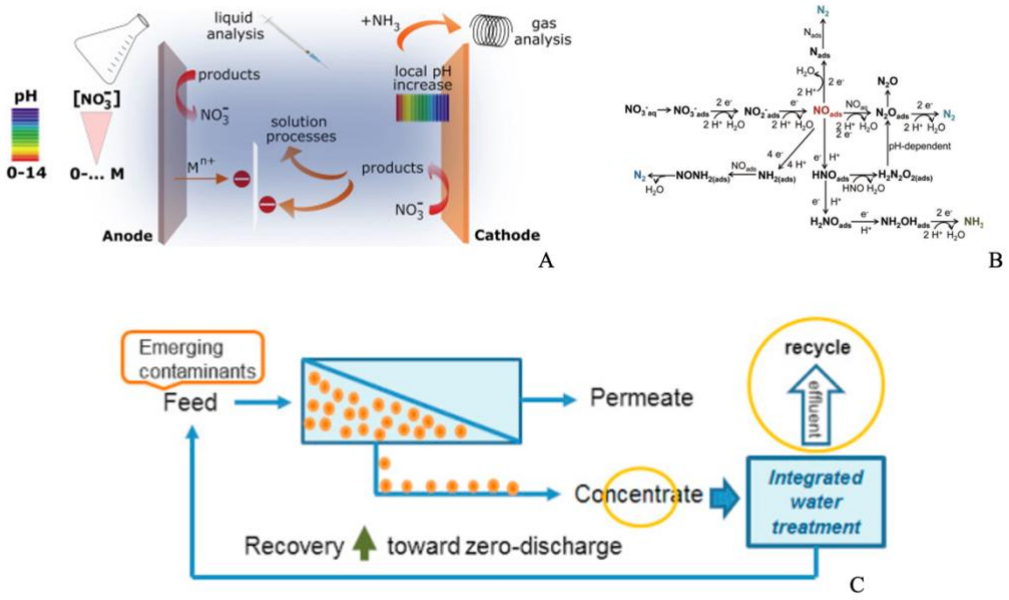

Figure 1. (**A**) Using electrocatalysts to assess the nitrate reduction rate (Katsounaros, 2021). (**B**) The electron-mediated pathway of nitrate electroreduction (Y. Wang et al., 2021). (**C**) The process of reverse osmosis treating wastewater (Joo & Tansel, 2015).

eutrophication in natural water bodies, an increase of heavy metals, and effect on soil quality (Petersen et al., 2018). Electrodialysis is a prominent post-treatment method for RO brine (C. Jiang et al., 2014). Others have tried to use natural evaporation and nanofiltration (NF) process as well (Ali, 2021; Arnal et al., 2005). Another difficulty that RO is experiencing is the high operating cost caused by the high applied pressure. The pressure varies from 2070 kPa to 10350 kPa (Kapoor & Viraraghavan, 1997) which not only casts a shadow on the overall cost but also tests the membrane performance. People usually add nanofiltration (NF) process as pretreatment before RO to reduce both the feed and brine concentration of RO (Epsztein et al., 2015). Membrane fouling is common sense in the membrane treatment process. The main fouling includes biofouling, organic fouling, inorganic fouling, and colloidal fouling (S. Jiang et al., 2017). These phenomena are more common in seawater distillation and wastewater treatment because the consistent of the raw water is much more complicated than groundwater.

The two primary ion exchange processes are selective ion exchange resins and electrodialysis. The mechanism of ion exchange process is to let the water pass through resin containing a strong base anion and the contaminant ions exchange with harmless ions in resins. Samatya et al. used nitrate-specific resins to treat polluted water and find that the removal rate increase with an increasing resin dose. The resins can be regenerated which makes the process more economical. Ion exchange, on the other hand, brings new ions into the solution. Although most of the newly added ions are harmless, the potential threat is still unknown. Electrodialysis can reach a high removal rate for contaminants and without introduce new ions. Elmidaoui et al. used electrodialysis to treat the nitrate in Moroccan groundwater. They came up with 95% of nitrate rejection and controlled the total cost in a relatively reasonable range. However, this technology still has a long way to go. The biggest barrier for

electrodialysis on a plant scale is the selectivity of the ion exchange membrane and the high equipment cost (Xu & Huang, 2008).

All the above separation procedures have one thing in common: requires brine post-treatment. The concentration of contaminants in brine are much higher than in the initial solution. In rural areas, wastewater won't be discharged into municipal pipeline instead it goes back to the aquifer and pollute the surface waters. Thus, the transformation of nitrate into ammonia or nitrogen becomes more critical (Figure 1B). Ammonia and nitrogen are the most stable products among nitrogen-containing species (Y. Wang et al., 2021). Chemical denitrification, electrocatalysis (Figure 1A) and biological denitrification make up the majority of nitrate transformation methods and they are often used for brine treatment. Chemical denitrification uses metals and their oxides to reduce the nitrate. Sabzali et al. removed nitrate from groundwater using zinc metal and sulfamic acid in electrolytic recovery reactors. They achieved a nearly 100% of nitrate removal and the remaining nitrate concentration was less than 1 mg L^{-1}. Kumar & Chakraborty used zero-valent magnesium (Mg^0) to convert nitrate into ammonia and nitrogen in aqueous solution. They achieved an 84% nitrate removal by finding out the suitable pH, temperature, and pressure when the initial NO_3^--N concentration was 50 mg L^{-1}. The biggest challenge for chemical denitrification is similar to ion exchange process. They all introduce new ions into the solution when this kind of phenomenon is not desired in most cases. As a result, electrocatalysis and biological denitrification are more widely studied recently.

Electrocatalysis denitrification is used for treating concentrate solution these days due to its high efficiency and don't need auxiliary chemicals. The mechanism for electrocatalysis is that nitrate gains electrons on the cathode side and converts to nitrate, ammonia, and nitrogen. Wang et al. used a three-dimensional Cu nanobelt cathode and reached over 95% nitrate reduction at 50 mg L^{-1}. Beltrame et al. used structured Pd

catalyst to reduce 76% of the nitrate in the solution which the initial concentration was 135.5 mg L^{-1} NO_3^--N. Beyond doubt, electrocatalysis has a bright future in large scale wastewater treatment. The formation of byproducts is the main concern for electrocatalysis, though the electrodes have high selectivity to form harmless products. Besides, there are still some other concerns including the cost of raw materials, energy consumption, and transportation. Biological denitrification is usually considered to be a heterotrophic process conducted by microorganisms (Gayle et al., 1989). The mechanism for this process is the heterotrophic denitrifying bacteria uses organic carbon sources to convert nitrate into nitrogen gas which don't need further treatment. The process involves the formation of nitrogen intermediates can be summarized as follows:

$$NO_3^- \rightarrow NO_2^- \rightarrow NO \rightarrow N_2O \rightarrow N_2$$

It is a well-developed technology and widely used in wastewater treatments plant after nitrification process. Moreover, biological denitrification may be the most economical strategy to treat nitrate polluted waters and wastewaters (Soares, 2000).

Microbial fuel cell (MFC)

Microbial fuel cell (MFC) is a system that uses bacteria as catalysts to oxidize organic and inorganic substances while also generate electrons (Logan et al., 2006). Most of the MFCs have two chambers: anode and cathode (Figure 2). The separator is the membrane that separates two chambers; it can be a cation, anion, or proton exchange membrane. The anode electrodes are usually made of carbon brush, fiber, and cloth. The bacterium was inoculated in the anode electrodes and consumed nutrients to produce proton and electrons (Min & Logan, 2004). The electrons are transferred to the cathode side through the wire. Today, the cathode usually uses Nafion as a Pt binder

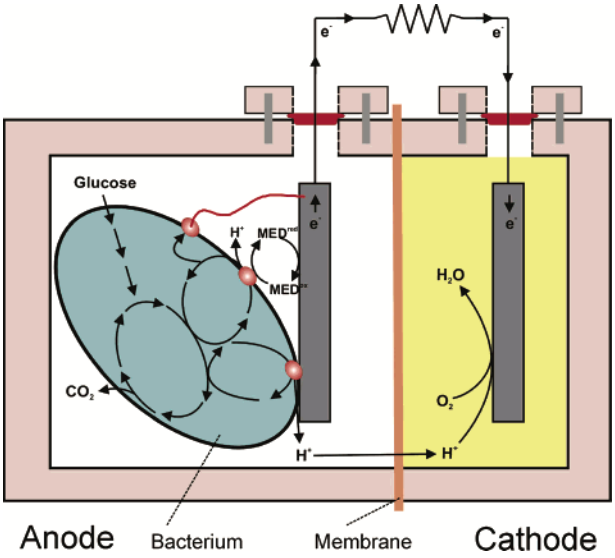

Figure 2. The most common structure of a dual-chamber microbial fuel cell (MFC) (Logan & Rabaey, 2012)

and activated carbon as Pb-catalyzed electrode to reach a higher power density (Cheng et al., 2006; F. Zhang et al., 2009). Oxygen serves as the electron acceptor at the cathode side. Although the acceptors can be various, oxygen is the most suitable one till now (Logan et al., 2006). To compensate that the cathode gaining electrons, the cations cross the cation exchange membrane and move from anode to cathode, or the anions go across the anion exchange membrane from cathode to anode. The main reactions inside MFC are below (Rahimnejad et al., 2015):

$$C_2H_4O_2 + 2H_2O \rightarrow 2CO_2 + 8e^- + 8H^+$$

$$2O_2 + 8H^+ + 8e^- \rightarrow 4H_2O$$

Biological denitrification uses bacteria which can convert nitrate and nitrite into gaseous products anaerobically. This nitrate removal technology is cheap and easy to operate. Furthermore, it is flexible to combine with other technologies to increase efficiency. To combine biological denitrification and MFC system, the nitrate removal microorganisms need to be inoculated in the electrode and act as the electron acceptor. C. Wang et al. combined Fenton oxidation and biological denitrification to treat toxic coking wastewater and reached 80% of COD removal and 78% removal of total nitrogen. Anoxic/oxic membrane bioreactor (A/O-MBR) is a typical membrane technology combined with biological denitrification. It can achieve a high COD and nitrate removal rate at the same time (Shen et al., 2009). There are also some examples to attach biological denitrification with MFC system. Clauwaert et al. used MFC to remove 0.146 kg NO_3^--N m^{-3} d^{-1} and a cell voltage of 0.075 V. Furthermore, J. Zhang et al. used anodic denitrification MFC reached a high denitrification rate.

The influence factors affecting the performance of MFC are various, including physical, biological, and process parameters. Electrodes and membrane characteristics affect the system output a lot. The output power is determined by the rate of substrate degradation, electron transfer, resistance, and performance of the electrode (Jung & Pandit, 2019). Researchers have been studying electrodes for years to discover more effective materials. Common separators include proton exchange membrane (PEM), cation exchange membrane (CEM) and anion exchange membrane (AEM). CEM is the most common used separator in MFC which transfer proton, but the competition from other cations makes the pH in cathode and anode varies (Jung & Pandit, 2019). AEM is also suitable as the separator for MFC system. Compared to CEM, AEM can achieve a higher power density (F. Zhang et al., 2009). Researchers find that AEM has a better performance than CEM because AEM can reduce the accumulation of proton and pH

splitting in two chambers (Kim et al., 2007). Selectivity is one of the most important characteristics of membrane. For AEM, the selectivity order is $Br^- > NO_3^- > Cl^- > F^-$, and the divalent anions can hardly go through the membrane (Epsztein et al., 2019; Luo et al., 2018). Although AEM is used widely in electrolytic cells and fuel cells, it is uncommon for MFC to use AEM as the separator because AEM has a higher substrate permeability which causes deformation of the membrane and increase of inner resistance.

The effectiveness of microorganisms influences the system performance in a large scale and is strongly determined by biological variables. Pure culture in MFCs have higher power output than mixed culture. This is mostly because mixed cultures require more time to form electroactive colonies on the anode (Sharma & Kundu, 2010). The operation factors including COD removal, current generation, and the biomass yield are influenced by the external resistance a lot. The biomass yield in the MFC is significantly less and COD removal is higher when external load is lower (Katuri et al., 2011). The effect of ionic strength will also be investigated. The higher the ionic strength is, the higher the power density is and the highest power density can reach 1 W m^{-2} (Liu et al., 2005).

People now use MFC in a variety of fields, including energy production, biohydrogen, wastewater treatment, and biosensor. While energy generation is still not the primary goal of MFC, the applications in wastewater treatment and biosensors are vast. Lorenzo et al. used MFC as a biosensor for biochemical oxygen demand (BOD_5) in wastewater and the sensor showed a good repeatability and consistent performance over a 7-month period. Zhuang et al. used air-cathode MFC to treat continuous real swine wastewater and got 77.1% of COD removal and 80.7% ammonia removal. Z. Li et al. used a two-chamber MFC to remove Cr^{6+} in real electroplating wastewater and 99.5% Cr^{6+} was

removed through the reduction process. Vilajeliu-Pons et al. used six-stacked scaled-up MFCs to treat swine manure which COD and total nitrogen (TN) load was high.

Some studies are focused more on nitrate removal by using MFC and there are two main nitrate removal processes. One is to set contaminated water as catholyte influent and microorganisms in the cathodic electrode, use heterotrophic or autotrophic denitrification to remove the nitrate (Figure 3). Vijay et al. studied nitrate removal using cow manure and soil using MFC and obtained a nitrate removal rate of 7.1 ± 0.9 kg NO_3^--N m^{-3} day^{-1}. Pous et al. used nitrate-polluted water as catholyte influent when both catholyte and anolyte were inoculated microorganisms and reached a denitrification rate of 75.7 ± 12.4 g NO_3^--N m^{-3} day^{-1}. The other one is to use polluted water as the anolyte influent, with heterotrophic denitrification occurring on the anode side. Ren et al. used a single-chamber MFC without pH buffer to treat different nitrate concentrations in the system and reached a 96% of nitrate reduction. Tong & He used AEM as a separator to treat groundwater as catholyte influent and the highest nitrate removal rate was 208.2 ± 13.3 g NO_3^--N m^{-3} day^{-1}.

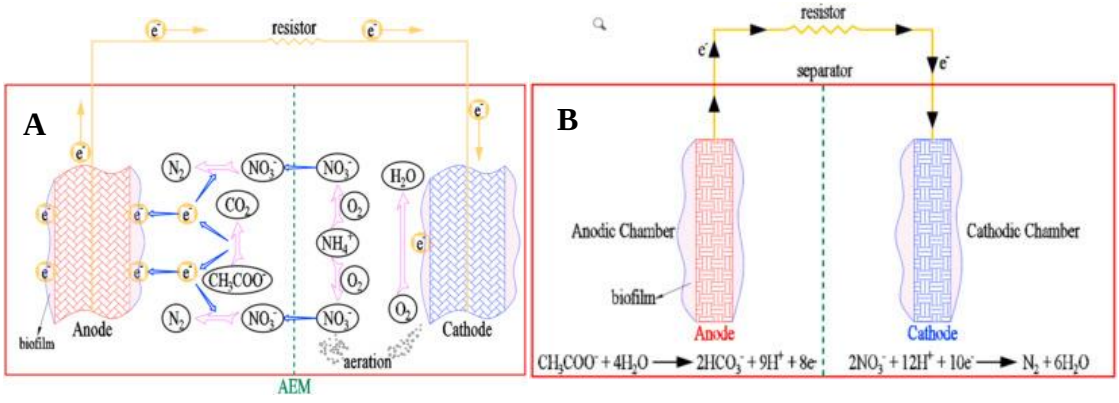

Figure 3. (**A**) Mechanism of heterotrophic anodic denitrification process in MFCs (**B**) Mechanism of nitrogen removal mechanism in an MFC with both cathode and anode inoculated with microorganisms (Nguyen & Babel, 2022)

MFC applications for nitrate removal in water treatment has a lot of advantages over conventional treatment process. D. Jiang et al. studied the MFC performance and tried to enhance the power production of a pilot-scale MFC. Dekker et al. analysis the MFC

performance with a total working volume of 20 L. However, because water treatment technology is currently quite established, it is difficult for the whole profession to embrace a new technique in a short period of time. Besides, there are still few MFC systems take into use in real water treatment process. Challenges are that following when everything become bigger, engineers need to deal with the reactor size, capital investment, and power management (W.-W. Li et al., 2013). According to studies, the most essential ways to assist MFC scale up are lowering internal resistance and finding a new separator to replace the ion exchange membrane. (Janicek et al., 2014).

Chapter 3: Materials and Methods

MFC setup

The dual-chamber MFC (Figure 4) was built by rectangular polycarbonate plates (12.7 cm * 17.78 cm * 0.635 cm McMaster-Carr, Chicago, IL, USA), separated by anion exchange membrane (AXM-100, Membranes International Inc., NJ, US). Rubber frames (12.7 cm * 7.62 cm * 1.27 cm) were inserted between each frame to ensure the tightness of the system. The net anodic and cathodic compartment volumes were 205 mL and 102.5 mL, respectively. Each chamber has an external reservoir to allow continuous recirculation in the system. The external reservoirs were continuously stirred by magnetic stirrers. The total volume of anolyte and catholyte is 500 mL and 600 mL separately. The cathode chamber was aerated with air (Figure 5). The solution flowed into the chamber's external reservoirs into the bottom of the chamber on both sides. This can make the solution be treated thoroughly and keep the anode chamber in anaerobic environment. The anode electrode was made from two 2.54 cm diameter carbon fiber brushes (The Mill-Rose Company, Mentor, OH, USA). The carbon brushes were soaked in acetone overnight, then dried in the fume hood and finally heated in the 450 ℃ ovens for 30 minutes. A carbon cloth cathode (area = 0.0039 m^2, Zoltek Companies, Inc., Bridgeton, MO, USA) electrode was coated with

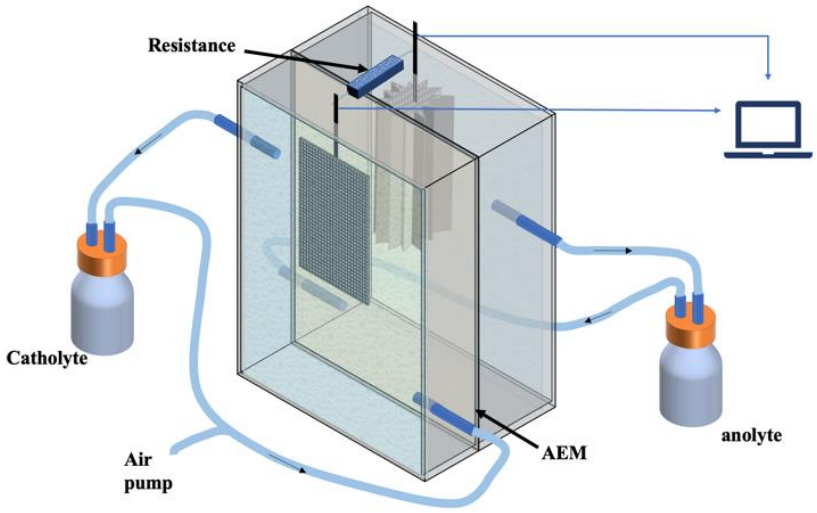

Figure 4. The diagrammatic sketch of experiment MFC system

Pt-carbon and supported by stainless steel mesh wire (F. Zhang et al., 2013). The carbon cloth was pretreated as carbon brushes. Besides, the carbon cloth was coated with Pt-carbon (10% wt/wt Pt/C, 2 mg cm^{-2}, Fuel Cell Earth, Woburn, MA, USA) and Nafion (10 μL mg^{-1} Pt-carbon, Fisher Scientific, US). The electrodes were connected to an external resistance by titanium wire to make a close circuit. The anode carbon brushes were inoculated with 15% mesophilic anaerobic digestion sludge (Nine Springs Wastewater Treatment Plant, Madison, WI, US). The microbes in the anode were fed with 1 g L^{-1} NaAc, 1 mL L^{-1} trace solution (Table 1), 10 mL L^{-1} stock solution (Table 2), and 10 mL L^{-1} Phosphate-Buffered Saline (PBS) (Table 3). The anode solution in reservoirs was changed once after the voltage drop to 1 mV. The system was operated under open circuit to allow the microbes grow up. After the voltage reached 700 mV steadily, external resistors were changed from open circuit to 10 Ω. The start-up condition was considered to end until the system run steadily after 2 months. All the experiments were carried out at laboratory temperature (22 ± 2 ℃). Cell voltages was monitored by computer and recorded every 300s using the Keithley Instruments (Tektronix, Inc., Beaverton, OR, USA).

Table 1. The recipe of trace solution

Chemical	Concentration/mg L^{-1}
$FeCl_2 \bullet 4H_2O$	10000
$CoCl_2 \bullet 6H_2O$	2000
EDTA Disodium Salt	1274.8
$MnCl_2 \bullet 4H_2O$	500
$NiCl_2 \bullet 6H_2O$	142
Na_2SeO_3	123
$ZnCl_2$	50
H_3BO_3	50
$CuCl_2 \bullet 2H_2O$	38
Concentrated HCl (mL)	1
$Na_2MoO_4 \bullet 2H_2O$	53.1758
$AlCl_3 \bullet 6H2O$	90

Table 2. The recipe of stock solution

Chemical	Concentration/g L^{-1}
NH_4Cl	15
NaCl	50
$MgSO_4 \bullet 7H_2O$	3.07153
$CaCl_2$	2
$NaHCO_3$	10

Table 3. The recipe of Phosphate-Buffered Saline (PBS)

Chemical	Concentration/g L^{-1}
K_2HPO_4	107
KH_2PO_4	53

Experiment procedure

During the experiments, all nitrate added in catholyte influent came from sodium nitrate and the chloride served as competing ions came from sodium chloride. Nine tests were performed, as summarized in Table 4. The nitrate concentration in Test 1 to 3 were 14 mg L^{-1}, 28 mg L^{-1}, 56 mg L^{-1} respectively. Tests 2, 4 and 5 were aimed at studying the effect of different catholyte chloride concentration ranging from 0 to 710 mg L^{-1} to nitrate removal. The effect of external resistance including 10 Ω, 470 Ω and open circuit was studied in Test 5 to 7. Test 8 used groundwater as catholyte to test the system performance. Test 9 conducted as a control to calculate the kinetics of biological denitrification. All tests are repeated for at least three cycles including two times of continuous sampling. In Test 2, 4 to 8, 28 mg L^{-1} NO_3^--N was introduced into the influent because it is about 3 times of the EPA standard. The solutions in both cathode and anode reservoirs were changed once after the voltage was under 1mV. For all anolyte solutions, 1 g L^{-1} NaAc, 10 mL L^{-1} stock solution, 10 mL L^{-1} Phosphate-Buffered Saline (PBS), and 1 mL L^{-1} trace solution were served as the nutrients for microbes. NaAc is the only source of substrate in anolyte. The recipe of stock solution, PBS, and trace solutions are showed on Table 1, Table 2, and Table 3. Anolyte solutions were purged with N_2 at least 10 minutes to remove the oxygen. All catholyte solutions all added 1mL L^{-1} PBS to maintain the pH. Dry chemicals used for the whole procedure were from Carolina Chemical (Charlotte, NC, USA), Alfa Aesar (Thermo Fisher Scientific, Tewksbury, MA, USA), and Sigma-Aldrich (Merck KGaA, Darmstadt, Germany).

Table 4. Summary of the operational condition of the experiments

Test	Anolyte	Catholyte	External resistance
1	/	14 mg L^{-1} NO_3^--N	10Ω
2	/	28 mg L^{-1} NO_3^--N	10Ω
3	/	56 mg L^{-1} NO_3^--N	10Ω
4	/	28 mg $L^{-1}$$NO_3^-$-N	10Ω
		142 mg L^{-1} Cl^-	
5	/	28 mg L^{-1} NO_3^--N	10Ω
		710 mg L^{-1} Cl^-	
6	/	28 mg L^{-1} NO_3^--N	470Ω
		710 mg L^{-1} Cl^-	
7	/	28 mg L^{-1} NO_3^--N	Open circuit
		710 mg L^{-1} Cl^-	
8	/	groundwater	10Ω
9	28 mg L^{-1} NO_3^--N	/	10Ω

Measurement and analysis

pH and conductivity among the experiment were measured via electrode probe and benchtop meter (Orion Versa Star Pro, Thermo Fisher Scientific, Waltham, MA, USA). Cl^- concentration was measured via Orio Chloride Electrodes and conductivity meter (Accumet research AR50, Fisher Scientific, Waltham, MA, USA). All solution samples were filtered through 0.45 μm PVDF membrane (HVLP02500, MilliporeSigma, US) before testing. Chemical oxygen demand (COD) and ammonia nitrogen (NH_3-N) were tested via standard colorimetric methods (COD Digestion Vials High Range, High Range Ammonia Nitrogen AmVer Salicylate Test 'N Tube, Hach, Loveland, CO, USA). The concentration of nitrate and nitrite were measured through high performance liquid chromatography (AT vp system, Shimadzu Scientific Instruments, Columbia, MD, USA). The groundwater samples were taken from an edge of field monitoring well adjacent to an agricultural field in Portage County, WI that typically grows a rotation of potato-field corn-peas-sweet corn. The ions in groundwater were test via inductively coupled plasma mass spectrometer (8900 triple quadrupole ICP-MS, Agilent, Santa Clara, CA, US) and ion chromatography (Thermo Dionex 1100/2100, Thermo Scientific, US)

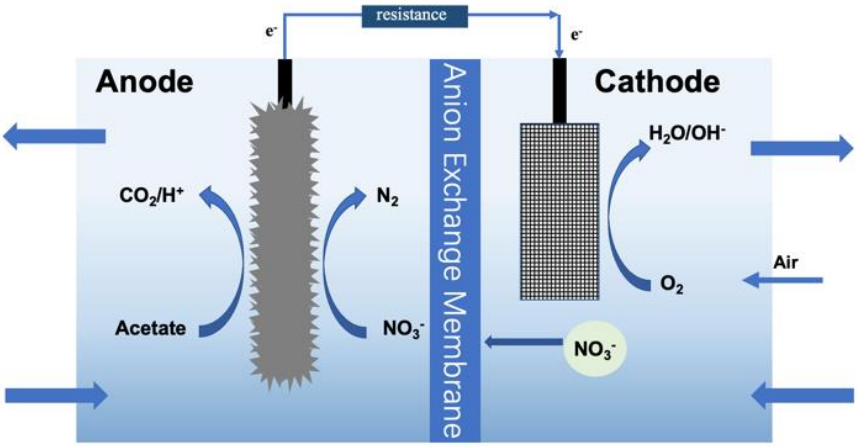

Figure 5. The cross-sectional sketch of experiment MFC system

Nitrate and COD removal rate was calculated as followed:

$$\text{Removal rate} = \frac{c_i - c_f}{c_i} \qquad \text{Eq. 1}$$

c_i is the initial concentration of COD in the anolyte or nitrate in the catholyte; c_f is the final concentration of COD in the anolyte or nitrate in the system.

Coulombic efficiency is the ratio of output (measured electricity) charge to the input charge (originated from organics):

$$\mathrm{CE} = \frac{Q_{out}}{Q_{in}} = \frac{\sum I \times t}{F \times \Delta COD \times V_{ano} \times \frac{1\ mol\ O_2}{32\ g\ O_2} \times \frac{4\ mol\ e^-}{1\ mol\ O_2}} \qquad \text{Eq. 2}$$

where $\sum I$ is the integration of current over the cycle, t is the time of the cycle, F is Faraday's constant, ΔCOD is the difference between initial and final, V_{ano} is the total volume of the anode liquid. Denitrification kinetics indicated the changes in activated sludge community metabolism. The carbon, energy substrate and the electron acceptors (in this case O_2) are in high concentration not to limit growth. Therefore, biological denitrification can be simplified into a zero-order kinetic model to describe the reactions (Glass & Silverstein, 1998). The kinetics of the whole system can be described using pseudo-first-order reaction. The following equation shows the relationship between the concertation and time in first-order reaction:

$$\mathrm{rate} = -\frac{dc}{dt} = \mathrm{kc} \qquad \text{Eq. 3}$$

$$\ln\left(\frac{c_i}{c_t}\right) = \mathrm{kt} \qquad \text{Eq. 4}$$

where c_i is the initial concentration of the nitrate in the catholyte, c_t is the concentration of the nitrate in the whole system at time t, and k is the reaction rate constant.

To characterize the performance of nitrate and chloride competitive behavior in the system, we used the selectivity of NO_3^- over Cl^- (C. He et al., 2018),

$$\rho\left(\frac{NO_3^-}{Cl^-}\right) = \frac{\Delta c_{NO_3^-}/c_{NO_3^-,0}}{\Delta c_{Cl^-}/c_{NO_3^-,0}} \qquad \text{Eq. 5}$$

In this equation, ρmeans the selectivity, $c_{i,0}$ is the initial concentration of the ions, Δc_i is the concentration difference between the calculated one and the initial.

Chapter 4: Results and discussion

Effect of NO_3^- concentrations in synthetic groundwater

In this section, we used synthetic groundwater to investigate the effect of nitrate concentration in the catholyte on nitrate removal in MFC reactor. 14 mg L^{-1}, 28 mg L^{-1}, and 56 mg L^{-1} of NO_3^--N were chosen to represent the different contamination levels since USEPA set MCL for NO_3^--N at 10 mg L^{-1} in drinking water. In some nitrate contaminated groundwater, the NO_3^--N concentration can be up to 40 mg L^{-1}. The external resistance, chloride concentration in catholyte influent and COD concentration were fixed at 10 Ω, 0 mg L^{-1}, and 600 mg L^{-1}, respectively.

Figure 6A shows the current profile of MFC under nitrate concentration varied from 14 mg L^{-1} to 56 mg L^{-1}. The maximum current was increased from 3.74 ± 0.25 mA to 5.86 ± 1.72 mA when the nitrate concentration increased from 14 mg L^{-1} to 28 mg L^{-1}, respectively. When the nitrate concentration was further increased to 56 mg L^{-1}, the maximum current dropped to 2.88 ± 0.59 mA. The trend for maximum current during each cycle was consistent with that for coulombic efficiency **(**Figure 6B and Table 5). The coulombic efficiency increased from 15.8 ± 6.4% to 22.8 ± 7.8% when the nitrate concentration increased from 14 mg L^{-1} to 28 mg L^{-1}, and decreased to 6.6 ± 5.3% when the concentration was 56 mg L^{-1}. The produced charge was also affected by the nitrate concentration. The charge was 571 ± 246 C when nitrate concentration was 14 mg L^{-1}, then increased to 815 ± 281 C at 28 mg L^{-1}, and finally dropped to 230 ± 24 C at 56 mg L^{-1}. The trend partially resulted from the change in current generation which was mentioned before. On the other hand, the produced charge was affected by cycle duration time. The cycle duration time was 2.2 ± 0.9 days, 1.6 ± 0.5 days, and 0.5 ± 0.6 days when the nitrate concentration was 14 mg L^{-1}, 28 mg L^{-1}, and 56 mg L^{-1}, respectively. The decreasing cycle duration time as the increase of nitrate concentration was also observed in a previous study, suggesting that the metabolism occurred between

denitrifying bacteria and electricity-generating bacteria for electron donor and improved bioelectrochemical activity (Jin et al., 2019).

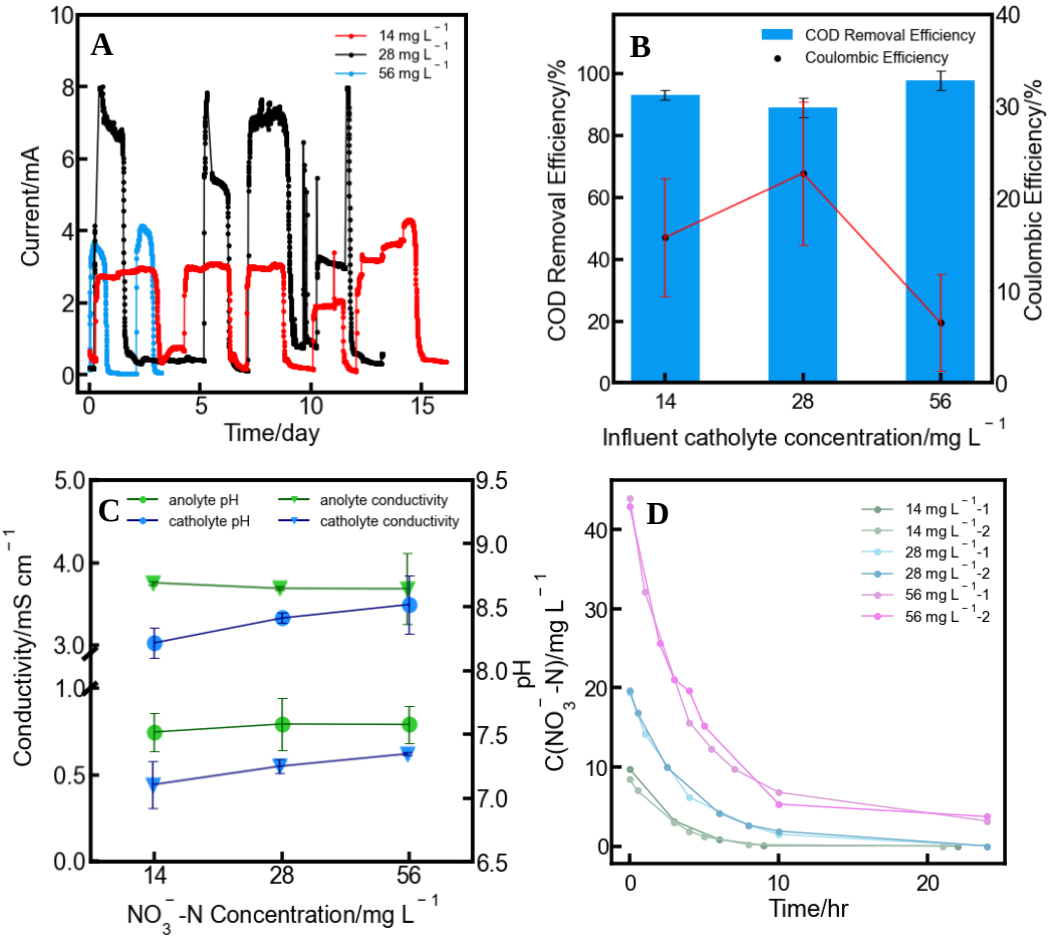

Figure 6. Performance of MFCs with NO_3^--N concentration of 14 mg L^{-1}, 28 mg L^{-1}, and 56 mg L^{-1} in the catholyte influent. (**A**) Current generation. (**B**) COD removal efficiency and coulombic efficiency. (**C**) pH and conductivity of the effluent from both anode chamber and cathode chamber. (**D**) The nitrate concentration profiles in catholyte as a function of time.

Table 5 shows the COD removal rate under different nitrate concentrations. Regardless of the nitrate concentration, we used in this section, the system had a high COD removal efficiency which was all above 88%, indicating that the COD removal was independent of the nitrate concentration. The change of pH values and conductivity in both anolyte and catholyte is illustrated in Figure 6C. The conductivity and pH values slightly changed on both sides with varying cathode nitrate concentrations. The catholyte

effluent conductivity increased while the conductivity of the anolyte effluent decreased, indicating that some anions in the anolyte were transported to the cathode side, driven by the concentration gradient. The pH of anolyte effluent remained constant due to the existence of PBS buffer. pH in catholyte effluent increased slightly from 8.22 ± 0.12 to 8.52 ± 0.23 as the increase of nitrate concentration in catholyte influent from 14 mg L^{-1} to 56 mg L^{-1}. This suggests that the concentration difference between Cl^- and Na^+ in the catholyte grew bigger. Though some anions came to cathode side, it was still not comparable to the number of NO_3^- move to anolyte.

Table 5. Nitrate removal, nitrate removal rate, COD removal efficiency, coulombic efficiency, and the produced charge under different nitrate concentration in catholyte influent

c(NO_3^--N)/mg L^{-1}	NO_3^--N removal/%	NO_3^--N removal rate/ mg L^{-1} hr^{-1}	COD removal efficiency/%	Coulombic efficiency/%	Produced charge/C
14	100	4.85 ± 1.18	93.0 ± 1.7	15.8 ± 6.4	572 ± 246
28	100	4.77 ± 0.14	89.0 ± 3.1	22.8 ± 7.8	815 ± 282
56	89.7 ± 1.5	8.28 ± 0.01	97.8 ± 3.1	6.6 ± 5.3	230 ± 24

Nitrate removal efficiency achieved 100% for both nitrate concentrations of 14 mg L^{-1} and 28 mg L^{-1}. The nitrate removal rate (Figure 6D) was 4.85 ± 1.18 mg L^{-1} hr^{-1} and 4.77 ± 0.14 mg L^{-1} hr^{-1} when the nitrate concentration was 14 mg L^{-1} and 28 mg L^{-1}, respectively. Further increase of nitrate concentration to 56 mg L^{-1} lead to a decreased nitrate removal efficiency of 89.7 ± 1.5% and an increased removal rate of 8.28 ± 0.01 mg L^{-1} hr^{-1}. The nitrate removal rate at 56 mg L^{-1} was 173% higher than that of 14 mg L^{-1} and 28 mg L^{-1}, which might be related to the COD/NO_3^--N ratio in the reactor. The COD/NO_3^--N ratio is defined as the concentration ratio of COD in the anolyte influent and the nitrate-nitrogen concentration in the catholyte influent. Here, the overall COD/NO_3^--N ratios were 42.8, 21.4, and 10.7 when the nitrate concentration was 14 mg L^{-1}, 28 mg L^{-1}, and 56 mg L^{-1}, respectively. Previous studies found that denitrification occurs most quickly when the COD/NO_3^--N ratio is between 7 and 12

(Vijay et al., 2016). Besides, the lower COD/NO_3^--N ratio in an anaerobic environment can promote denitrification activity (Akunna et al., 1992; Ruiz et al., 2006). The denitrifiers can hardly be detected under a high COD/ NO_3^--N ratio which suggests that nitrate removal is limited by the absence of denitrifies under a high COD/ NO_3^--N ratio (Akunna et al., 1992). In our experiments, only when nitrate concentration was 56 mg L^{-1}, the ratio falls in the best COD/NO_3^--N for MFC system. This explained why when nitrate removal rate reached the maximum at the initial concentration was 56 mg L^{-1} in influent.

The change in CE and the number of generated charges were caused by the varying activity of bacterial communities under different nitrate concentrations. The presence of nitrate might inhibit the activity of electrochemically active microorganisms, resulting in low CE and produced charge at 14 mg L^{-1} which needs further confirmation. Furthermore, the comparatively low nitrate concentration resulted in no dominating genus of denitrifying bacteria in the system. When nitrate concentration increased to 28 mg L^{-1}, the denitrifying bacteria become more active. Some denitrifying bacteria not only participate in the denitrification, but also produce electricity (Jin et al., 2018). These bacteria continued to consume acetate even after the denitrification process was completed. Instead, they used the substrate to generate power causing the rise of CE and produced charge. When the nitrate concentration was raised from 28 mg L^{-1} to 56 mg L^{-1}, the COD concentration remained constant while the CE decreased dramatically. The organic compounds were employed to support the activity of electrochemically-active microbes, denitrifying bacteria and others (Sukkasem et al., 2008). When the nitrate concentration was higher, denitrifying bacteria consumed more substrate whereas electrochemically active microorganisms consumed less, resulting in a fall in CE.

We note that the highest nitrate removal rate in the experiment was still lower than that in previous studies. J. Zhang et al. used an anodic denitrification microbial fuel cell (AD-MFC) and reached a high denitrification capacity of 52.5 mg L^{-1} hr^{-1}. Davarpanah et al. used an up-flow tubular MFC to treat groundwater and achieved a maximum nitrate removal rate of 10.4 mg L^{-1} hr^{-1}. All these studies involved a heterotrophic denitrification process in anolyte which is the same as this experiment. Most prior research treated nitrate-contaminated water by directly feeding it into the anode chamber for heterotrophic denitrification, but in our work, we put the nitrate-rich synthetic groundwater into the cathode chamber. The advantage of feeding contaminated groundwater to the cathode chamber is that it is purely a physicochemical process for the groundwater stream without any interference generated during the biological process. However, since the nitrate ions need to be transported across the ion exchange membrane, it added another step for nitrate separation from the synthetic groundwater before the denitrification process. Hence, the nitrate removal rate was hindered by the separation step and lower than that in MFCs fed with nitrate-rich water in the anode chamber. We note that the transport of nitrate ions across the membrane may be the limiting step in the MFC system.

Feeding nitrate-rich groundwater into the anode

To study how the transmembrane transport of nitrate ions affects the nitrate removal in MFC, we also directly fed synthetic groundwater with 28 mg L^{-1} NO_3^--N into the anode chamber. The COD removal rate was 97.8 ± 0.1%, slightly higher than that in MFC with the same concentration of nitrate fed into the cathode chamber. The conductivity of catholyte and anolyte effluent were 0.44 ± 0.04 mS cm^{-1} and 3.89 ± 0.03 mS cm^{-1}, respectively. The pH of the catholyte and anolyte effluent were 8.44 ± 0.06 and 7.43 ± 0.05, respectively. All effluent pH and conductivity were comparable to the situation that nitrate concentration was 28 mg L^{-1} in catholyte (Table 6).

Table 6. pH and conductivity when nitrate concentration was 28 mg L^{-1} in catholyte and anolyte influent

c(NO_3^--N)/mg L^{-1}	NO_3^--N removal/%	NO_3^--N removal rate/ mg L^{-1} hr^{-1}	COD removal efficiency/%	Coulombic efficiency/%	Produced charge/C
28	100	23.38 ± 12.01	97.8 ± 0.1	6.8 ± 0.8	232 ± 32

Table 7. Nitrate removal, nitrate removal rate, COD removal efficiency, coulombic efficiency, and the produced charge when nitrate set as anolyte influent

Nitrate influent	Catholyte pH	Anolyte pH	Catholyte Conductivity/mS cm^{-1}	Anolyte Conductivity/mS cm^{-1}
Catholyte	7.43 ± 0.05	8.44 ± 0.06	0.44 ± 0.04	3.89 ± 0.03
Anolyte	7.58 ± 0.21	8.41 ± 0.04	0.55 ± 0.04	3.69 ± 0.03

Table 7 shows the system performance when the nitrate concentration was 28 mg L^{-1} in anolyte influent. The coulombic efficiency was 6.8 ± 0.8 % and the produced charge was 232 ± 32 C, both comparable to the data obtained from MFC fed with 56 mg L^{-1} nitrate concentration as catholyte influent (6.6 ± 5.3% and 230 ± 24 C). The biological

denitrification reached 100% during the batch cycle. However, the MFC fed with 28 mg L^{-1} NO_3^--N into the anode had a nitrate removal rate of 23.38 ± 12.01 mg L^{-1} hr^{-1}, much higher than that from reactor with 28 mg L^{-1} NO_3^--N into the cathode (~5 mg L^{-1} hr^{-1}), demonstrating that the nitrate removal rate is not governed solely by biological denitrification. When nitrate-rich water was fed into the cathode chamber, the nitrate removal rate is affected by both anion mass transfer across the membrane and the biological denitrification in the anode chamber. Because the simple denitrification rate is substantially faster than the total removal rate, the biological denitrification rate, a zero-order process, is no longer the limit step. Nitrate mass transfer is divided into three stages: diffusion, migration, and convection. The solution flow direction in the system was parallel to the membrane. As a result, the convection component contributes little and may be omitted. Ion migration is not the main driving force. The high removal rate of nitrate and COD in open circuit further demonstrated that migration had little impact on the overall process. In addition, the anolyte was mixed with stock solution, PBS, and trace solution. These solutions all delivered electrolytes with substantially larger concentrations of other ions than nitrate and acetate. As a result, the determining factor for nitrate movement, in this case, is diffusion.

Effect of chloride concentration in synthetic groundwater

We also investigated the effect of competing ions on nitrate removal in MFC. Chloride was selected as a model competing ion in the catholyte influent, with concentration varying from 0 mg L^{-1} to 710 mg L^{-1}. The concentration of nitrate, COD, anolyte chloride concentration, and external resistance were fixed at 28 mg L^{-1}, 600 mg L^{-1}, 600 mg L^{-1}, and 10 Ω, respectively. Although other anions such as PO_4^{3-}, $H_2PO_4^-$, and SO_4^{2-} were present in the anolyte, they were not considered as competitive ions in the systems due to their low concentration and low diffusion rate through AEM.

Table 8. Nitrate removal, nitrate removal rate, COD removal efficiency, coulombic efficiency, and the charge under different influent cathode chloride concentration

$c(Cl^-)$/mg L^{-1}	NO_3^--N removal/%	NO_3^--N removal rate/ mg L^{-1} hr^{-1}	COD removal efficiency/%	Coulombic efficiency/%	Produced charge/C
0	100	4.77 ± 0.14	89.0 ± 3.1	22.8 ± 7.8	815 ± 282
142	100	4.57 ± 0.01	92.4 ± 6.6	26.2 ± 9.2	913 ± 309
710	97.84 ± 2.2	2.41 ± 0.45	89.5 ± 2.4	19.5 ± 4.1	692 ± 143

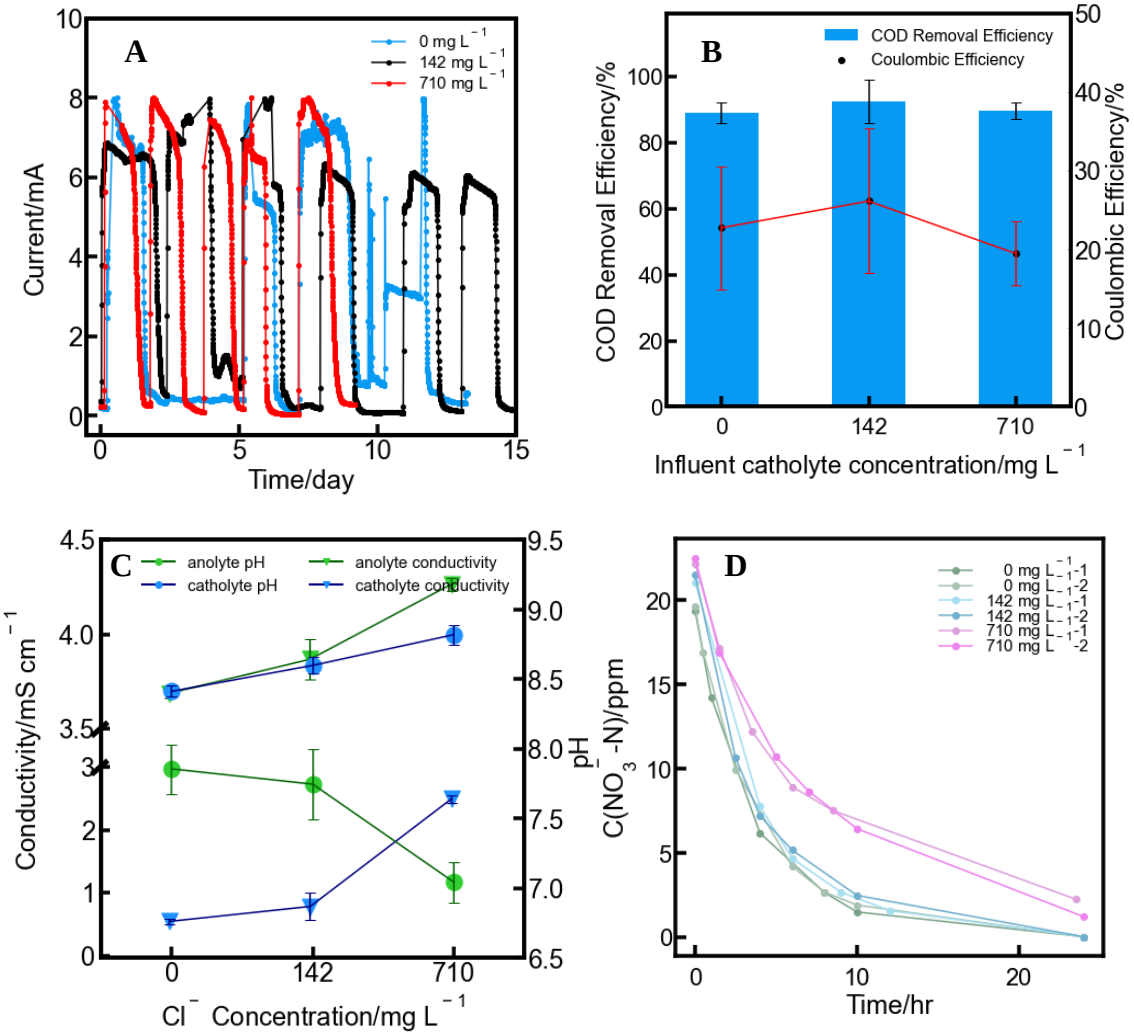

Figure 7. Performance of MFCs with Cl- concentration of 0 mg L^{-1}, 142 mg L^{-1}, and 710 mg L^{-1} in the catholyte influent (**A**) Current generation. (**B**) COD removal efficiency and coulombic efficiency. (**C**) pH and conductivity of the effluent from both anode chamber and cathode chamber. (**D**) The nitrate concentration profiles in catholyte as a function of time.

Figure 7A shows the system's current profile at varying chloride concentrations. The maximum current was 5.85 ± 1.72 mA, 6.42 ± 0.61 mA, and 7.16 ± 0.19 mA when the chloride concentration was 0 mg L^{-1}, 142 mg L^{-1} and 710 mg L^{-1}, respectively. The higher maximum current was generated when chloride concentration was 710 mg L^{-1}, which might be attributed to the increase of ionic strength with more NaCl in the catholyte.

Table 8 illustrates the system performance under different influent cathode chloride concentrations. The CE of the system was 22.8 ± 7.8%, 26.2 ± 9.2 %, and 19.5 ± 4.1%

when the chloride concentration of catholyte influent was 0 mg L^{-1}, 142 mg L^{-1}, and 710 mg L^{-1}, respectively. The produced charges followed the same trend as CE, which was 815 ± 282 C, 913 ± 309 C, and 692 ± 143 C as the chloride concentration increased from 0 to 710 mg L^{-1}. There was no significant difference in CE or produced charge between 0 mg L^{-1} and 142 mg L^{-1} chloride concentration. However, at high chloride concentration of 710 mg L^{-1}, there was a modest drop in both CE and the quantity of produced charges. This resulted from the restricted bacterial activity in anode chamber by the high chloride concentration. As shown in Figure 7B, the system achieved a high COD removal efficiency, the overall COD removal efficiency exceeded 88%. The conductivity of both chambers increased with the increase in chloride concentration. The catholyte conductivities were 0.55 ± 0.04 mS cm^{-1}, 0.79 ± 0.22 mS cm^{-1}, and 2.49 ± 0.06 mS cm^{-1} when the chloride concentration was 0 mg L^{-1}, 142 mg L^{-1}, and 710 mg L^{-1}, respectively. At the same time, the anolyte conductivities ranged from 3.69 ± 0.03 mS cm^{-1}, 3.87 ± 0.11 mS cm^{-1}, to 4.27 ± 0.03 mS cm^{-1}. pH in catholyte effluent increased from 8.41 ± 0.04 to 8.82 ± 0.07 when the chloride concentration increased from 0 mg L^{-1} to 710 mg L^{-1}, respectively. pH of catholyte and anolyte influent was fixed at 7.79 ± 0.10 and 7.78 ± 0.11, respectively (Figure 7C). In contrast, pH in anolyte decreased with the increase of chloride concentration. The decrease of pH in anolyte and the increase of pH in catholyte both resulted from the movement of chloride in two chambers. When the chloride concentration was 0 mg L^{-1} and 142 mg L^{-1}, PBS in both chambers can offset the pH change caused by the movement of chloride ions in an extent. However, when the concentration of chloride increased to 710 mg L^{-1}, the chloride concentration was substantially higher than in anolyte (Figure 7B). At the same time, while the quantity of cations remained constant in all situations, there was a difference between cations and anions, which resulted in a reduction in pH. The overall nitrate removal, which was 100% at 0 mg L^{-1} and 142 mg L^{-1} chloride concentrations, decreased to 97.8 ± 2.2 % at a high chloride concentration which was 710 mg L^{-1}. This

phenomenon demonstrated that high chloride concentrations impeded bacterial action, resulting in a reduction in nitrate removal (Venkata Mohan et al., 2014).

At a constant COD and nitrate concentration, the nitrate removal efficiency fluctuated when the chloride concentration changed. The anolyte influent chloride concentration was fixed at 600 mg L^{-1}. When the chloride concentration in catholyte influent (0 and 142 mg L^{-1}) was lower than that in the anolyte (600 mg L^{-1}), the nitrate removal rate was 4.77 ± 0.14 mg L^{-1} hr^{-1} and 4.57 ± 0.01 mg L^{-1} hr^{-1} (Figure 7D). The removal rate decreased to 2.41 ± 0.45 mg L^{-1} hr^{-1} when the chloride concentration increased to 710 mg L^{-1} in the catholyte, twice lower than that in low chloride concentration (0 mg L^{-1} and 142 mg L^{-1}). The heterotrophic denitrification process can be described as the following four reduction steps (Gregory et al., 2004):

$$NO_3^- + 2e^- + 2H^+ \rightarrow NO_2^- + H_2O$$

$$NO_2^- + e^- + 2H^+ \rightarrow NO + H_2O$$

$$NO + e^- + H^+ \rightarrow 0.5N_2O + H_2O$$

$$0.5N_2O + e^- + H^+ \rightarrow 0.5N_2 + 0.5H_2O$$

During the whole tests, there was no nitrite left in both catholyte and anolyte effluent indicating that the rate which nitrate converts to nitrite is exceedingly quick although the chloride concentration different among experiments.

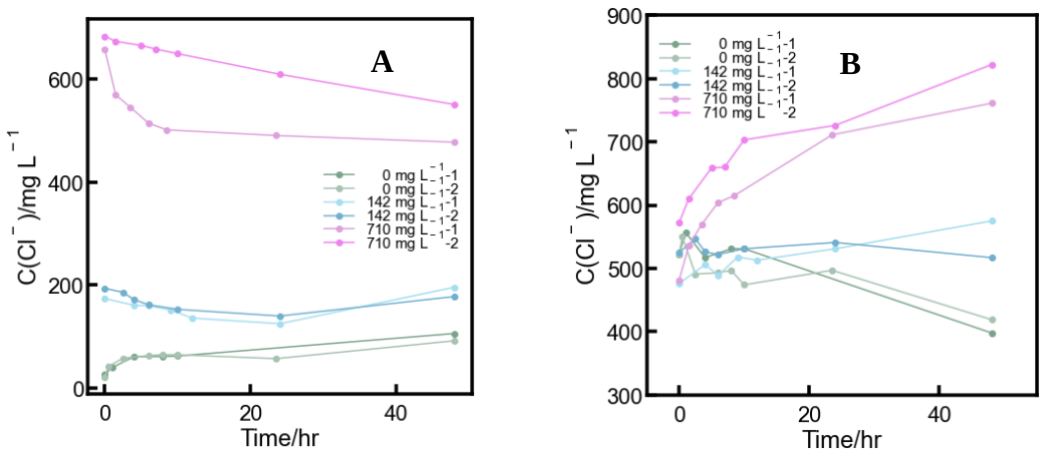

Figure 8. Cl^- concentration of 0 mg L^{-1}, 142 mg L^{-1}, and 710 mg L^{-1} in the catholyte influent (**A**) In catholyte change over time (**B**) In anolyte change over time

Moreover, the final anolyte chloride concentration varied among the experiments despite no significant change in influent concentration (Figure 8A-B). The final chloride concentration in anolyte was 408.5 ± 14.9 mg L^{-1}, 546.0 ± 41.0 mg L^{-1}, 791.5 ± 43.1 mg L^{-1} when the influent chloride concentration in catholyte was 0 mg L^{-1}, 142 mg L^{-1}, 710 mg L^{-1}, respectively. At the same time, the final chloride concentration also ranged from 99.0 ± 10.0 mg L^{-1} to 187.1 ± 12. 7 mg L^{-1} to 514.5 ± 51.6 mg L^{-1} as the chloride concentration rose. The cause of the concentration difference was complicated. The nitrate and acetate were consumed throughout the process. The anion exchange membrane acted as a separator, preventing cations from crossing the membrane. As a result, Na^+ remained on both sides of the solution. However, the masses of sodium nitrate and sodium acetate were different, which was 1.2 mmol and 6 mmol, respectively. This indicates that following the reaction, the amount of cations in anolyte is always greater than that in catholyte. As a result, the anion moved across the AEM to balance the charge.

Table 9. The selectivity of nitrate to chloride in catholyte

$c(Cl^-)$/mg L^{-1}	142 mg L^{-1}	710 mg L^{-1}
$\rho(NO_3^-/Cl^-)$	3.57 ± 0.02	3.52

Table 9 shows the selectivity of nitrate to chloride in catholyte. Although the catholyte influent chloride concentration difference, the selectivity was close, indicating the chloride concentration barely has effect on nitrate movement in this system. In microbial fuel cell system, the selectivity is a result of the combination of electromigration and diffusion. As we discussed before, the main driving force for nitrate movement is diffusion. When the chloride concentration in anolyte and catholyte influent was 600 mg L^{-1} and 710 mg L^{-1}, the final concentrations in anolyte and catholyte were 791.5 ± 43.1 mg L^{-1} and 514.5 ± 51.6 mg L^{-1}, respectively. The chloride concentration distribution was affected by electromigration. If the chloride

concentration distribution was only affected by the concentration gradient, the final concentration of the chloride should be close in two chambers. However, the discrepancy was there. This indicating that the driving force for chloride ions were includes electromigration. However, the proportion of effect from concentration gradient and electromigration was unknown. To find out the relationship between diffusion and electromigration needs further experiments.

Effect of external resistance

In this section, we will illustrate the effect of current generation on nitrate removal from synthetic groundwater. The external resistance was manipulated to three levels: 10 Ω, 470 Ω, and quasi-infinite (open circuit mode). COD, chloride, and nitrate concentration was set at 600 mg L^{-1}, 28 mg L^{-1}, and 710 mg L^{-1}, respectively. The influent chloride concentration was fixed at 710 mg L^{-1} to simulate the groundwater contaminated by road salt. Road salt is commonly used for road deicing in northern regions, resulting in the contamination of chloride in groundwater (Williams et al., 2000).

Table 10. Nitrate removal, nitrate removal rate, COD removal rate, and coulombic efficiency of the system when external resistance different

External resistance	NO_3^--N removal efficiency/%	NO_3^--N removal rate/ mg L^{-1} hr^{-1}	COD removal/%	Coulombic efficiency/%
10Ω	97.8 ± 2.2	2.38 ± 0.50	89.5 ± 2.4	19.5 ± 4.1
470Ω	100	2.96 ± 0.53	96.3 ± 4.9	3.25 ± 2.2
Open circuit	92.4 ± 1.1	2.18 ± 0.39	94.7 ± 2.1	/

Figure 9A shows the current profile under 10 Ω, 470 Ω, and quasi-infinite external resistances. The maximum voltage were 0.07 ± 0.02 V, 0.42 ± 0.01 V, and 0.74 ± 0.02 V, respectively. The voltage was stable in open circuit mode because the electrons produced by exoelectrogens were accumulated at the anode and were incapable of being transported to the cathode, making the potential difference between the two electrodes barely change. The maximum current reached 7.16 ± 0.19 mA when the external resistance was 10 Ω, and dropped to 0.89 ± 0.01 mA at 470 Ω. Furthermore, the system reached a high CE of 19.5 ± 4.1 % when the external resistance was 10 Ω. The CE was only 3.2 ± 2.2 % with 470 Ω external resistance. The coulombic efficiency was lower at 470 Ω compared with that of 10 Ω, illustrating that the majority of the substrate was

not used for current generation under high external resistance (470 Ω). Instead, a certain amount of electron donor was competed by electrogenic bacteria, fermentative, and anaerobically respiring organisms (Katuri et al., 2011). Besides, the coulombic efficiency reached its highest when the external resistance is near to the internal resistance which means the inner resistance of the system is closer to 10 Ω instead of 470 Ω (Pinto et al., 2011).

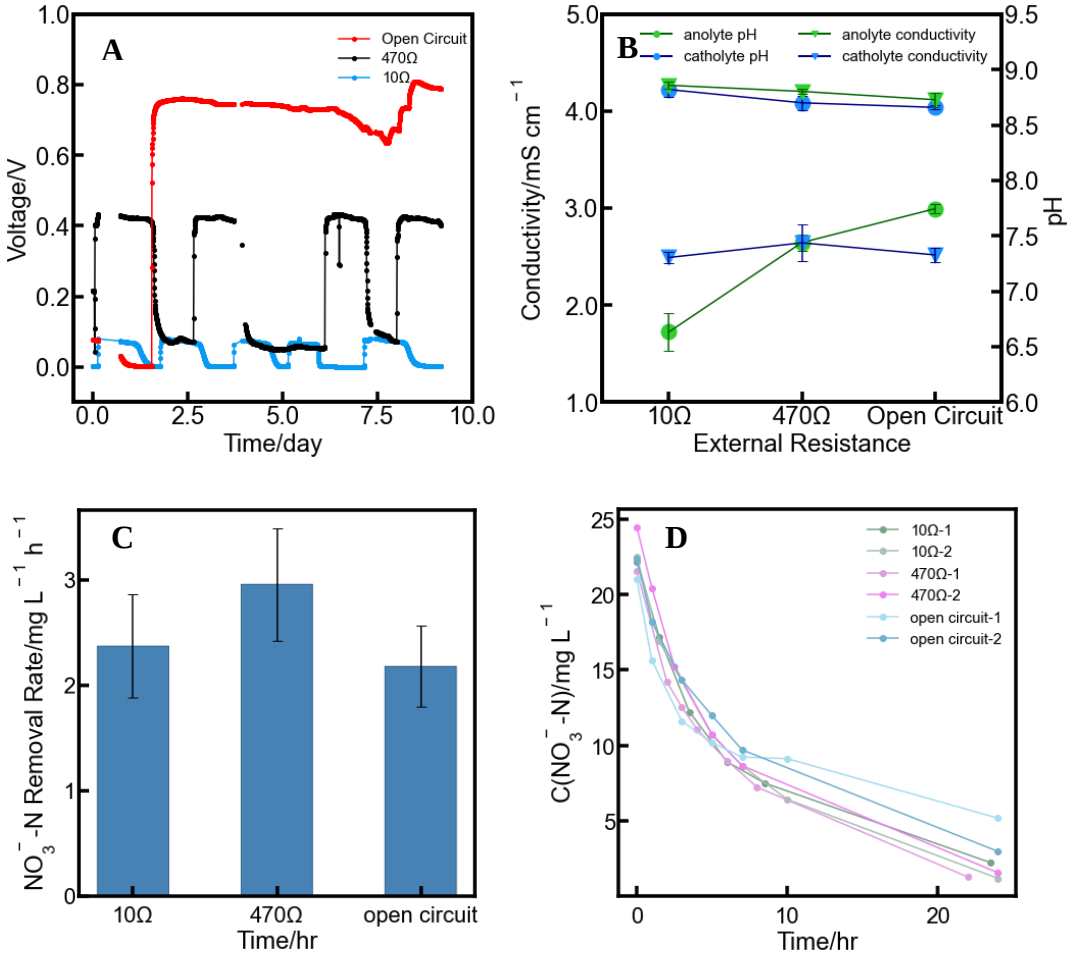

Figure 9. Performance of MFCs with external resistance of 10 Ω, 470 Ω, and open circuit (**A**) Current generation. (**B**) pH and conductivity of the effluent from both anode chamber and cathode chamber. (**C**) The nitrate removal rate (**D**) The nitrate concentration profiles in catholyte as a function of time.

When it comes to the removal efficiency of COD, there is no significant variation between different external resistances. The COD removal rate changed from 89.5 ± 2.4 % to 96.3 ± 4.9 % when the external resistance was 10 Ω and 470 Ω, respectively,

suggesting that COD removal efficiency was not affected by the current generation. The conductivity of both anolyte and catholyte remained stable regardless of the external resistance connected to the reactor (Figure 9B). The pH of anolyte effluent was decreased to 6.63 ± 0.17 when the resistor was 10 Ω, 14% lower than that at open circuit. We think that the pH variation was mainly due to the transport of chloride ions. Because the system was using AEM as a separator which only allows anion to cross the membrane, Na^+ remained where it was. Simultaneously, the chloride ions migrate due to electromigration or a concentration gradient. The pH difference between the two chambers was created by an imbalance in the quantity of cations and anions. During the experiments, only the solutions in the reservoirs changed which means half of the former solution was still in chamber and mixed with the new one. As a result, this might make the accumulation of chloride in chamber as time passed.

The nitrate removal efficiency (Figure 9C and Table 10) and removal rate (Figure 9D) were slightly different when the external resistance was different. We didn't observe a big difference in nitrate removal efficiency and its removal rate when the resistor was 10 Ω and 470 Ω. The heterotrophic denitrification process consumes the electrons. Though the external resistance is different, the microorganisms still provide enough electrons for the denitrification process. Even while there was no substantial reduction

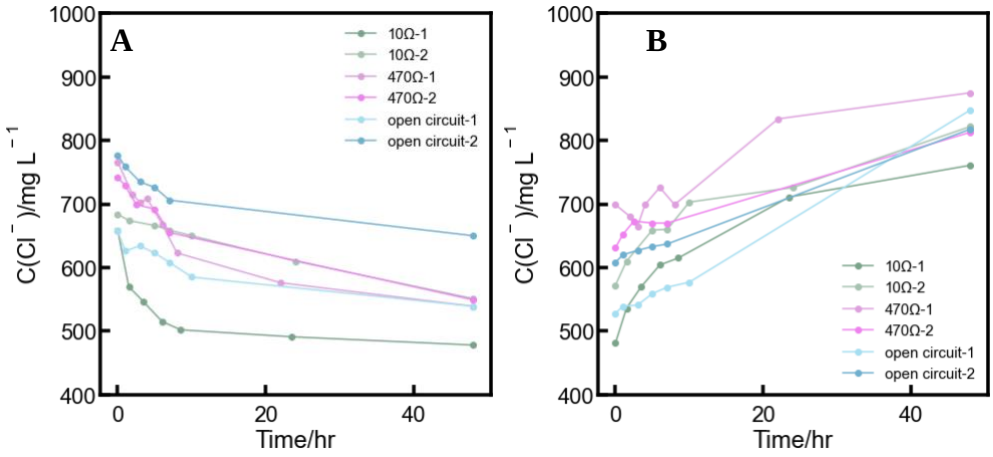

Figure 10. (**A**) The chloride concentration in catholyte changed over time when the external resistance different (**B**) The chloride concentration in anolyte changed over time when the external resistance different

in COD removal efficiency at open circuit, a little drop in nitrate removal rate which was 2.18 ± 0.39 mg L^{-1} hr^{-1} was observed. The removal efficiency was 92.4 ± 1.1 % without resistor which was 5% lower than that of 10 Ω. According to research, when MFC was in open-circuit mode, electrogenic bacteria were less prevalent in the anode and more *Archaea* were present (Fang et al., 2013). COD was competed between denitrification bacteria, electrogenic bacteria and others for metabolism. Simultaneously, the nitrate removal efficiency was still high, indicating the electrons from electron-generating bacteria were still enough for denitrification process. The production of methane is possible because the nitrate was not fully removed in open circuit which meant that the electron acceptors were various during the process. The overall finding is that external resistance has little effect on MFC system performance, including COD and nitrate removal rate. Because the anodic biofilm community may alter depending on the environment, demonstrating MFC's adaptability. The findings were similar to the previous study in that open circuit did not affect nitrate removal (Lyon et al., 2010).

Even though the external resistances vary, the trend of the chloride concentration changes was similar. The concentration of chloride dropped on the cathode side while increasing on the anode side during the whole process **(**Figure 10A-B). The anolyte and catholyte chloride concentrations were 551.0 ± 55.5 mg L^{-1} and 789.5 ± 114.3 mg L^{-1}, respectively. Because of the concentration gradient, nitrate migrated from the catholyte to the anolyte and was subsequently consumed on the anode side. Because the sodium acetate was used as COD, and acetate was consumed when sodium remained. Due to the permselectivity order for anion transport through AEM, nitrate transports before chloride (Epsztein et al., 2019; Luo et al., 2018). As a result, the nitrate first went across the anion exchange membrane than chloride. After acetate and nitrate reached their removal limit, the concentration of anions and cations stayed constant in both anolyte and catholyte. Besides, there is no more current which means the electromigration

disappeared and the concentration distribution of other ions in two chambers simply depends on Donnan Dialysis.

Nitrate removal from real groundwater

To evaluate the system performance for real groundwater treatment, experiments were conducted using real groundwater samples as catholyte. The groundwater sample was collected from an edge of field monitoring well adjacent to an agricultural field in Portage County, WI that typically grew a rotation of potato-field corn-peas-sweet corn. It contains Na^{+}, Ca^{2+}, K^{+}, Mg^{2+} for cations and NO_3^{-}, Cl^{-}, SO_4^{2-}, PO_4^{3-} for anions. The concentration of NO_3^{-}-N in this groundwater was 44.52 mg L^{-1} and the chloride concentration was 70 mg L^{-1}. The total organic carbon in groundwater was 5.73 mg L^{-1}. The pH and conductivity of the groundwater was 8.116 and 0.775 mS cm^{-1}, respectively. The groundwater was fed as catholyte，and the microbes in the anode were fed with 1 g L^{-1} NaAc, 10 ml L^{-1} stock solution, 10 mL L^{-1} Phosphate-Buffered Saline (PBS), and 1 mL L^{-1} trace solution. Anolyte and Catholyte changed once the voltage dropped to 10 mV. The external resistance was 10 Ω. The duration time of cycles reached 1.3 ± 0.1 days which was higher than when the system was fed with synthetic groundwater with a nitrate concentration of 56 mg L^{-1} (0.5 ± 0.6 days). The COD removal efficiency reached 98.2 ± 3.1%. When the catholyte influent was groundwater, the system reached a coulombic efficiency of 6.2 ± 0.5 % and coulombic charge was 231 ± 38 C which were similar to the experiment when the nitrate concentration was 56 mg L^{-1} (230 ± 24 C). The nitrate removal efficiency was 90.6 ± 12.1 % and the removal rate was 5.4 ± 0.7 mg L^{-1} hr^{-1} which was similar to the simulated one. This demonstrated that the system is efficient for nitrate removal from groundwater.

Chapter 5: Conclusion

This study evaluated the effect of nitrate and chloride concentrations, as well as current generation, on nitrate removal in MFC with simulated and genuine nitrate-rich groundwater. When the nitrate content varied from 14 mg L^{-1} to 56 mg L^{-1} under various operation conditions, most of the experiments demonstrated a high nitrate removal effectiveness of better than 95%. The nitrate removal rate related to the ratio of COD/ NO_3^--N. The nitrate removal rate increased to 8.28 ± 0.01 mg L^{-1} hr^{-1} when the catholyte influent concentration raised to 56 mg L^{-1}. Microorganism activity was inhibited by high nitrate concentration (56 mg L^{-1}) resulting in a reduction in coulombic efficiency. The nitrate removal mechanism in this system mainly primarily comprised of two sequential processes: diffusion from anode side to cathode and biological denitrification in the anolyte. The heterotrophic denitrification is a zero-order reaction when nitrate removal reaction in the whole system act as a pseudo-first-order reaction, among which the diffusion speed is the limiting step of the whole nitrate removal process. Moreover, nitrate removal is also affected by the concentration of competing ions. A high concentration of competing chloride (710 mg L^{-1}) limits the activity of bacteria and resulted in a decreased nitrate removal efficiency and rate. The selectivity of nitrate to chloride in catholyte was constant and unaffected by chloride concentration. The chloride concentration in anolyte and catholyte were changed with different current and chloride influent concentration. As a result, both electromigration and diffusion are the driving forces behind the movement of chloride ions. This MFC system also achieved a 90.6 ± 12.1 % nitrate removal and 5.4 ± 0.7 mg L^{-1} hr^{-1} removal rate when treating actual groundwater. The current generation barely influences nitrate removal in the system. The system behaved differently under different conditions implying that the domain bacteria community is different. Overall, the microbial fuel cell is a promising technique for both in-situ groundwater treatment as well as wastewater treatment. MFC, on the other hand, is still on a laboratory scale. Some of the critical factors in the system still need further understanding. Besides, ions in actual groundwater are much more

complicated than synthetic ones when the conductivity is relatively low. Whether these factors will affect the system also needs further study. Finally, the cost of MFC remains an issue. Though the membrane segment, which accounts for a substantial percentage of the cost, is not required in the cell, it can improve system performance on a big scale.

References

Akunna, J. C., Bizeau, C., & Moletta, R. (1992). Denitrification in anaerobic digesters: Possibilities and influence of wastewater COD/N-NO x ratio. *Environmental Technology*, *13*(9), 825–836. https://doi.org/10.1080/09593339209385217

Ali, M. E. A. (2021). Nanofiltration Process for Enhanced Treatment of RO Brine Discharge. *Membranes*, *11*(3), 212. https://doi.org/10.3390/membranes11030212

Almasri, M. N. (2007). Nitrate contamination of groundwater: A conceptual management framework. *Environmental Impact Assessment Review*, *27*(3), 220–242. https://doi.org/10.1016/j.eiar.2006.11.002

Archna, Sharma, S. K., & Sobti, R. C. (2012). Nitrate Removal from Ground Water: A Review. *E-Journal of Chemistry*, *9*(4), 1667–1675. https://doi.org/10.1155/2012/154616

Arnal, J. M., Sancho, M., Iborra, I., Gozálvez, J. M., Santafé, A., & Lora, J. (2005). Concentration of brines from RO desalination plants by natural evaporation. *Desalination*, *182*(1–3), 435–439. https://doi.org/10.1016/j.desal.2005.02.036

Beltrame, T. F., Zoppas, F. M., Gomes, M. C., Ferreira, J. Z., Marchesini, F. A., & Bernardes, A. M. (2021). Electrochemical nitrate reduction of brines: Improving selectivity to N2 by the use of Pd/activated carbon fiber catalyst. *Chemosphere*, *279*, 130832. https://doi.org/10.1016/j.chemosphere.2021.130832

Bijay-Singh, & Craswell, E. (2021). Fertilizers and nitrate pollution of surface and ground water: An increasingly pervasive global problem. *SN Applied Sciences*, *3*(4), 518. https://doi.org/10.1007/s42452-021-04521-8

Cheng, S., Liu, H., & Logan, B. E. (2006). Power Densities Using Different Cathode Catalysts (Pt and CoTMPP) and Polymer Binders (Nafion and PTFE) in Single Chamber Microbial Fuel Cells. *Environmental Science & Technology*, *40*(1), 364–369. https://doi.org/10.1021/es0512071

Clauwaert, P., Rabaey, K., Aelterman, P., De Schamphelaire, L., Pham, T. H., Boeckx, P., Boon, N., & Verstraete, W. (2007). Biological Denitrification in Microbial Fuel Cells. *Environmental Science & Technology*, *41*(9), 3354–3360. https://doi.org/10.1021/es062580r

Davarpanah, L., Sarbisheh, F., & Sharghi, E. A. (2020). A novel process of anodic water denitrification in an upflow tubular microbial fuel cell: Effect of C/N ratio. *Journal of Chemical Technology & Biotechnology*, *95*(12), 3179–3192. https://doi.org/10.1002/jctb.6496

Dekker, A., Heijne, A. T., Saakes, M., Hamelers, H. V. M., & Buisman, C. J. N. (2009). Analysis and Improvement of a Scaled-Up and Stacked Microbial Fuel Cell. *Environmental Science & Technology*, *43*(23), 9038–9042. https://doi.org/10.1021/es901939r

Dieter, C.A., Maupin, M.A., Caldwell, R.R., Harris, M.A., Ivahnenko, T.I., Lovelace, J.K., Barber, N.L., & Linsey, K.S. (2017). *Estimated use of water in the United States in 2015: U.S. Geological Survey Circular 1441*. (Circular) [Circular].

Elmidaoui, A., Elhannouni, F., Menkouchi Sahli, M. A., Chay, L., Elabbassi, H., Hafsi, M., & Largeteau, D. (2001). Pollution of nitrate in Moroccan ground water: Removal by electrodialysis. *Desalination*, *136*(1–3), 325–332. https://doi.org/10.1016/S0011-9164(01)00195-3

Epsztein, R., Nir, O., Lahav, O., & Green, M. (2015). Selective nitrate removal from groundwater using a hybrid nanofiltration–reverse osmosis filtration scheme. *Chemical Engineering Journal*, *279*, 372–378. https://doi.org/10.1016/j.cej.2015.05.010

Epsztein, R., Shaulsky, E., Qin, M., & Elimelech, M. (2019). Activation behavior for ion permeation in ion-exchange membranes: Role of ion dehydration in selective transport. *Journal of Membrane Science*, *580*, 316–326. https://doi.org/10.1016/j.memsci.2019.02.009

Fang, Z., Song, H.-L., Cang, N., & Li, X.-N. (2013). Performance of microbial fuel cell coupled constructed wetland system for decolorization of azo dye and bioelectricity generation. *Bioresource Technology*, *144*, 165–171. https://doi.org/10.1016/j.biortech.2013.06.073

Gayle, B. P., Boardman, G. D., Sherrard, J. H., & Benoit, R. E. (1989). Biological Denitrification of Water. *Journal of Environmental Engineering*, *115*(5), 930–943. https://doi.org/10.1061/(ASCE)0733-9372(1989)115:5(930)

Genders, J. D., Hartsough, D., & Hobbs, D. T. (1996). Electrochemical reduction of nitrates and nitrites in alkaline nuclear waste solutions. *Journal of Applied Electrochemistry*, *26*(1), 1–9. https://doi.org/10.1007/BF00248182

Glass, C., & Silverstein, J. (1998). Denitrification kinetics of high nitrate concentration water: PH effect on inhibition and nitrite accumulation. *Water Research*, *32*(3), 831–839. https://doi.org/10.1016/S0043-1354(97)00260-1

Gregory, K. B., Bond, D. R., & Lovley, D. R. (2004). Graphite electrodes as electron donors for anaerobic respiration. *Environmental Microbiology*, *6*(6), 596–604. https://doi.org/10.1111/j.1462-2920.2004.00593.x

Hansen, B., Thorling, L., Schullehner, J., Termansen, M., & Dalgaard, T. (2017). Groundwater nitrate response to sustainable nitrogen management. *Scientific Reports*, *7*(1), 8566. https://doi.org/10.1038/s41598-017-07147-2

He, C., Ma, J., Zhang, C., Song, J., & Waite, T. D. (2018). Short-Circuited Closed-Cycle Operation of Flow-Electrode CDI for Brackish Water Softening. *Environmental Science & Technology*, *52*(16), 9350–9360. https://doi.org/10.1021/acs.est.8b02807

He, H., Huang, Y., Yan, M., Xie, Y., & Li, Y. (2020). Synergistic effect of electrostatic adsorption and ion exchange for efficient removal of nitrate. *Colloids and Surfaces A: Physicochemical and Engineering Aspects*, *584*, 123973. https://doi.org/10.1016/j.colsurfa.2019.123973

Janicek, A., Fan, Y., & Liu, H. (2014). Design of microbial fuel cells for practical application: A review and analysis of scale-up studies. *Biofuels*, *5*(1), 79–92. https://doi.org/10.4155/bfs.13.69

Jiang, C., Wang, Y., Zhang, Z., & Xu, T. (2014). Electrodialysis of concentrated brine from RO plant to produce coarse salt and freshwater. *Journal of Membrane Science*, *450*, 323–330. https://doi.org/10.1016/j.memsci.2013.09.020

Jiang, D., Curtis, M., Troop, E., Scheible, K., McGrath, J., Hu, B., Suib, S., Raymond, D., & Li, B. (2011). A pilot-scale study on utilizing multi-anode/cathode microbial fuel cells (MAC MFCs) to enhance the power production in wastewater treatment. *International Journal of Hydrogen Energy*, *36*(1), 876–884. https://doi.org/10.1016/j.ijhydene.2010.08.074

Jiang, S., Li, Y., & Ladewig, B. P. (2017). A review of reverse osmosis membrane fouling and control strategies. *Science of The Total Environment*, *595*, 567–583. https://doi.org/10.1016/j.scitotenv.2017.03.235

Jin, X., Guo, F., Liu, Z., Liu, Y., & Liu, H. (2018). Enhancing the Electricity Generation and Nitrate Removal of Microbial Fuel Cells With a Novel Denitrifying Exoelectrogenic Strain EB-1. *Frontiers in Microbiology*, *9*, 2633. https://doi.org/10.3389/fmicb.2018.02633

Jin, X., Guo, F., Ma, W., Liu, Y., & Liu, H. (2019). Heterotrophic anodic denitrification improves carbon removal and electricity recovery efficiency in microbial fuel cells. *Chemical Engineering Journal*, *370*, 527–535. https://doi.org/10.1016/j.cej.2019.03.023

Jung, S. P., & Pandit, S. (2019). Important Factors Influencing Microbial Fuel Cell Performance. In *Microbial Electrochemical Technology* (pp. 377–406). Elsevier. https://doi.org/10.1016/B978-0-444-64052-9.00015-7

Kang, G., & Cao, Y. (2012). Development of antifouling reverse osmosis membranes for water treatment: A review. *Water Research*, *46*(3), 584–600. https://doi.org/10.1016/j.watres.2011.11.041

Kapoor, A., & Viraraghavan, T. (1997). Nitrate Removal From Drinking Water—Review. *Journal of Environmental Engineering*, *123*(4), 371–380. https://doi.org/10.1061/(ASCE)0733-9372(1997)123:4(371)

Katuri, K. P., Scott, K., Head, I. M., Picioreanu, C., & Curtis, T. P. (2011). Microbial fuel cells meet with external resistance. *Bioresource Technology*, *102*(3), 2758–2766. https://doi.org/10.1016/j.biortech.2010.10.147

Kikhavani, T., Ashrafizadeh, S. N., & Van der Bruggen, B. (2014). Nitrate Selectivity and Transport Properties of a Novel Anion Exchange Membrane in Electrodialysis. *Electrochimica Acta*, *144*, 341–351. https://doi.org/10.1016/j.electacta.2014.08.012

Kim, J. R., Cheng, S., Oh, S.-E., & Logan, B. E. (2007). Power Generation Using Different Cation, Anion, and Ultrafiltration Membranes in Microbial Fuel Cells. *Environmental Science & Technology*, *41*(3), 1004–1009. https://doi.org/10.1021/es062202m

Konikow, L. F. (2011). Contribution of global groundwater depletion since 1900 to sea-level rise: GROUNDWATER DEPLETION. *Geophysical Research Letters*, *38*(17), n/a-n/a. https://doi.org/10.1029/2011GL048604

Kumar, M., & Chakraborty, S. (2006). Chemical denitrification of water by zero-valent magnesium powder. *Journal of Hazardous Materials*, *135*(1–3), 112–121. https://doi.org/10.1016/j.jhazmat.2005.11.031

Li, W.-W., Yu, H.-Q., & He, Z. (2013). Towards sustainable wastewater treatment by using microbial fuel cells-centered technologies. *Energy Environ. Sci.*, *7*(3), 911–924. https://doi.org/10.1039/C3EE43106A

Li, Z., Zhang, X., & Lei, L. (2008). Electricity production during the treatment of real electroplating wastewater containing Cr6+ using microbial fuel cell. *Process Biochemistry*, *43*(12), 1352–1358. https://doi.org/10.1016/j.procbio.2008.08.005

Liu, H., Cheng, S., & Logan, B. E. (2005). Power Generation in Fed-Batch Microbial Fuel Cells as a Function of Ionic Strength, Temperature, and Reactor Configuration. *Environmental Science & Technology*, *39*(14), 5488–5493. https://doi.org/10.1021/es050316c

Logan, B. E., Hamelers, B., Rozendal, R., Schröder, U., Keller, J., Freguia, S., Aelterman, P., Verstraete, W., & Rabaey, K. (2006). Microbial Fuel Cells: Methodology and Technology. *Environmental Science & Technology*, *40*(17), 5181–5192. https://doi.org/10.1021/es0605016

Logan, B. E., & Rabaey, K. (2012). Conversion of Wastes into Bioelectricity and Chemicals by Using Microbial Electrochemical Technologies. *Science*, *337*(6095), 686–690. https://doi.org/10.1126/science.1217412

Logan, B. E., Rossi, R., Ragab, A., & Saikaly, P. E. (2019). Electroactive microorganisms in bioelectrochemical systems. *Nature Reviews Microbiology*, *17*(5), 307–319. https://doi.org/10.1038/s41579-019-0173-x

Lorenzo, M. D., Curtis, T. P., Head, I. M., & Scott, K. (2009). A single-chamber microbial fuel cell as a biosensor for wastewaters. *Water Research*, 10.

Luo, T., Abdu, S., & Wessling, M. (2018). Selectivity of ion exchange membranes: A review. *Journal of Membrane Science*, *555*, 429–454. https://doi.org/10.1016/j.memsci.2018.03.051

Lyon, D. Y., Buret, F., Vogel, T. M., & Monier, J.-M. (2010). Is resistance futile? Changing external resistance does not improve microbial fuel cell performance. *Bioelectrochemistry*, *78*(1), 2–7. https://doi.org/10.1016/j.bioelechem.2009.09.001

Majumdar, D., & Gupta, N. (2000). Nitrate pollution of groundwater and associated human health disorders. *Indian Journal of Environmental Health*.

Malaeb, L., & Ayoub, G. M. (2011). Reverse osmosis technology for water treatment: State of the art review. *Desalination*, *267*(1), 1–8. https://doi.org/10.1016/j.desal.2010.09.001

Mechenich, D. (2015). *Interactive Well Water Quality Viewer 1.0. University of Wisconsin-Stevens Point, Center for Watershed Science and Education.* http://www.uwsp.edu/cnr-ap/watershed/Pages/WellWaterViewer.aspx

Min, B., & Logan, B. E. (2004). Continuous Electricity Generation from Domestic Wastewater and Organic Substrates in a Flat Plate Microbial Fuel Cell.

Environmental Science & Technology, *38*(21), 5809–5814. https://doi.org/10.1021/es0491026

Petersen, K. L., Paytan, A., Rahav, E., Levy, O., Silverman, J., Barzel, O., Potts, D., & Bar-Zeev, E. (2018). Impact of brine and antiscalants on reef-building corals in the Gulf of Aqaba – Potential effects from desalination plants. *Water Research*, *144*, 183–191. https://doi.org/10.1016/j.watres.2018.07.009

Pinto, R. P., Srinivasan, B., Guiot, S. R., & Tartakovsky, B. (2011). The effect of real-time external resistance optimization on microbial fuel cell performance. *Water Research*, *45*(4), 1571–1578. https://doi.org/10.1016/j.watres.2010.11.033

Pous, N., Puig, S., Coma, M., Balaguer, M. D., & Colprim, J. (2013). Bioremediation of nitrate-polluted groundwater in a microbial fuel cell: Bioremediation of nitrate-polluted groundwater in a microbial fuel cell. *Journal of Chemical Technology & Biotechnology*, *88*(9), 1690–1696. https://doi.org/10.1002/jctb.4020

Qasim, M., Badrelzaman, M., Darwish, N. N., Darwish, N. A., & Hilal, N. (2019). Reverse osmosis desalination: A state-of-the-art review. *Desalination*, *459*, 59–104. https://doi.org/10.1016/j.desal.2019.02.008

Rahimnejad, M., Adhami, A., Darvari, S., Zirepour, A., & Oh, S.-E. (2015). Microbial fuel cell as new technology for bioelectricity generation: A review. *Alexandria Engineering Journal*, *54*(3), 745–756. https://doi.org/10.1016/j.aej.2015.03.031

Ren, Y., Lv, Y., Wang, Y., & Li, X. (2020). Effect of heterotrophic anodic denitrification on anolyte pH control and bioelectricity generation enhancement of bufferless microbial fuel cells. *Chemosphere*, *257*, 127251. https://doi.org/10.1016/j.chemosphere.2020.127251

Rezvani, F., Sarrafzadeh, M.-H., Ebrahimi, S., & Oh, H.-M. (2019). Nitrate removal from drinking water with a focus on biological methods: A review. *Environmental Science and Pollution Research*, *26*(2), 1124–1141. https://doi.org/10.1007/s11356-017-9185-0

Ruiz, G., Jeison, D., & Chamy, R. (2006). Development of denitrifying and methanogenic activities in USB reactors for the treatment of wastewater: Effect of COD/N ratio. *Process Biochemistry*, *41*(6), 1338–1342. https://doi.org/10.1016/j.procbio.2006.01.007

Sabzali, A., Gholami, M., Yazdanbakhsh, A. R., Khodadadi, A., Musavi, B., & Mirzaee, R. (2006). *CHEMICAL DENITRIFICATION OF NITRATE FROM GROUNDWATER VIA SULFAMIC ACID AND ZINC METAL*. *3*(3), 6.

Sahoo, P. K., Kim, K., & Powell, M. A. (2016). Managing Groundwater Nitrate Contamination from Livestock Farms: Implication for Nitrate Management Guidelines. *Current Pollution Reports*, *2*(3), 178–187. https://doi.org/10.1007/s40726-016-0033-5

Samatya, S., Kabay, N., Yüksel, Ü., Arda, M., & Yüksel, M. (2006). Removal of nitrate from aqueous solution by nitrate selective ion exchange resins. *Reactive and Functional Polymers*, *66*(11), 1206–1214. https://doi.org/10.1016/j.reactfunctpolym.2006.03.009

Schoeman, J. J., & Steyn, A. (2003). Nitrate removal with reverse osmosis in a rural area in South Africa. *Desalination*, *155*(1), 15–26. https://doi.org/10.1016/S0011-9164(03)00235-2

Sharma, V., & Kundu, P. P. (2010). Biocatalysts in microbial fuel cells. *Enzyme and Microbial Technology*, *47*(5), 179–188. https://doi.org/10.1016/j.enzmictec.2010.07.001

Shen, J., He, R., Han, W., Sun, X., Li, J., & Wang, L. (2009). Biological denitrification of high-nitrate wastewater in a modified anoxic/oxic-membrane bioreactor (A/O-MBR). *Journal of Hazardous Materials*, *172*(2–3), 595–600. https://doi.org/10.1016/j.jhazmat.2009.07.045

Soares, M. I. M. (2000). Biological Denitrification of Groundwater. In S. Belkin (Ed.), *Environmental Challenges* (pp. 183–193). Springer Netherlands. https://doi.org/10.1007/978-94-011-4369-1_16

Sukkasem, C., Xu, S., Park, S., Boonsawang, P., & Liu, H. (2008). Effect of nitrate on the performance of single chamber air cathode microbial fuel cells. *Water Research*, *42*(19), 4743–4750. https://doi.org/10.1016/j.watres.2008.08.029

Tong, Y., & He, Z. (2013). Nitrate removal from groundwater driven by electricity generation and heterotrophic denitrification in a bioelectrochemical system. *Journal of Hazardous Materials*, *262*, 614–619. https://doi.org/10.1016/j.jhazmat.2013.09.008

Venkata Mohan, S., Velvizhi, G., Annie Modestra, J., & Srikanth, S. (2014). Microbial fuel cell: Critical factors regulating bio-catalyzed electrochemical process and recent advancements. *Renewable and Sustainable Energy Reviews*, *40*, 779–797. https://doi.org/10.1016/j.rser.2014.07.109

Vijay, A., Vaishnava, M., & Chhabra, M. (2016). Microbial fuel cell assisted nitrate nitrogen removal using cow manure and soil. *Environmental Science and Pollution Research*, *23*(8), 7744–7756. https://doi.org/10.1007/s11356-015-5934-0

Vilajeliu-Pons, A., Puig, S., Salcedo-Dávila, I., Balaguer, M. D., & Colprim, J. (2017). Long-term assessment of six-stacked scaled-up MFCs treating swine manure with different electrode materials. *Environmental Science: Water Research & Technology*, *3*(5), 947–959. https://doi.org/10.1039/C7EW00079K

Wang, C., Liu, Y., Huang, M., Xiang, W., Wang, Z., Wu, X., Zan, F., & Zhou, T. (2022). A rational strategy of combining Fenton oxidation and biological processes for efficient nitrogen removal in toxic coking wastewater. *Bioresource Technology*, *363*, 127897. https://doi.org/10.1016/j.biortech.2022.127897

Wang, X., Zhu, M., Zeng, G., Liu, X., Fang, C., & Li, C. (2020). A three-dimensional Cu nanobelt cathode for highly efficient electrocatalytic nitrate reduction. *Nanoscale*, *12*(17), 9385–9391. https://doi.org/10.1039/C9NR10743F

Wang, Y., Wang, C., Li, M., Yu, Y., & Zhang, B. (2021). Nitrate electroreduction: Mechanism insight, *in situ* characterization, performance evaluation, and challenges. *Chemical Society Reviews*, *50*(12), 6720–6733. https://doi.org/10.1039/D1CS00116G

Ward, M., Jones, R., Brender, J., de Kok, T., Weyer, P., Nolan, B., Villanueva, C., & van Breda, S. (2018). Drinking Water Nitrate and Human Health: An Updated Review. *International Journal of Environmental Research and Public Health*, *15*(7), 1557. https://doi.org/10.3390/ijerph15071557

Williams, D. D., Williams, N. E., & Cao, Y. (2000). Road salt contamination of groundwater in a major metropolitan area and development of a biological index to monitor its impact. *Water Research*, *34*(1), 127–138. https://doi.org/10.1016/S0043-1354(99)00129-3

Wisconsin Groundwater Coordinating Council (GCC). (2022). *Wisconsin Groundwater Coordinating Council Report to the Legislature* (p. 21).

Xu, T., & Huang, C. (2008). Electrodialysis-based separation technologies: A critical review. *AIChE Journal*, *54*(12), 3147–3159. https://doi.org/10.1002/aic.11643

Zhang, F., Cheng, S., Pant, D., Bogaert, G. V., & Logan, B. E. (2009). Power generation using an activated carbon and metal mesh cathode in a microbial fuel cell. *Electrochemistry Communications*, *11*(11), 2177–2179. https://doi.org/10.1016/j.elecom.2009.09.024

Zhang, F., Ge, Z., Grimaud, J., Hurst, J., & He, Z. (2013). Long-Term Performance of Liter-Scale Microbial Fuel Cells Treating Primary Effluent Installed in a Municipal Wastewater Treatment Facility. *Environmental Science & Technology*, *47*(9), 4941–4948. https://doi.org/10.1021/es400631r

Zhang, J., Zheng, P., Zhang, M., Chen, H., Chen, T., Xie, Z., Cai, J., & Abbas, G. (2013). Kinetics of substrate degradation and electricity generation in anodic denitrification microbial fuel cell (AD-MFC). *Bioresource Technology*, *149*, 44–50. https://doi.org/10.1016/j.biortech.2013.09.043

Zhuang, L., Zheng, Y., Zhou, S., Yuan, Y., Yuan, H., & Chen, Y. (2012). Scalable microbial fuel cell (MFC) stack for continuous real wastewater treatment. *Bioresource Technology*, *106*, 82–88. https://doi.org/10.1016/j.biortech.2011.11.019